

INFLUENCE OF MAGNETIC FIELD EXPOSURE AND CLAY MINERAL ADDITION ON  
THE FRACTIONATION OF GREEK YOGURT WHEY COMPONENTS

by

CLINTON KYLE

B.S., Kansas State University, 2013

B.S., Kansas State University, 2013

A THESIS

submitted in partial fulfillment of the requirements for the degree

MASTER OF SCIENCE

Food Science

KANSAS STATE UNIVERSITY  
Manhattan, Kansas

2015

Approved by:

Major Professor  
Jayendra Amamcharla

# **Copyright**

CLINTON KYLE

2015

## Abstract

Greek yogurt is one of the largest-growing sectors in the dairy industry accounting for over 25% of yogurt sales in the United States. Greek yogurt is produced by removing a portion of water and water soluble components from yogurt. Consequently, a large quantity of Greek yogurt whey (GYW) is being produced as a co-product. GYW is compositionally different from cheese whey, and thus poses economic and environmental challenges to the dairy industry. The objective of the present study was to evaluate two physical treatments as alternative methods for separating valuable GYW components: magnetic fluid treatment (MFT) and the addition of sepiolite, a clay mineral. A MFT chamber was designed using four pairs of neodymium magnets arranged to produce a magnetic field strength of 0.6 Tesla. Three batches of GYW each from two manufacturers were procured. A 2×3 factorial design was used with MFT or without MFT and the addition of zero, two, or four grams of sepiolite per 100g of GYW. The pH of GYW was adjusted to 7.2 using 5N NaOH solution, and the GYW was pumped at a rate of 7.5 L/min through the MFT system with or without MFT chamber attached. The sample was split into three sub-samples, heated to 80°C, and sepiolite was added as per the experimental design. The samples were centrifuged at 1,000g for five minutes. The top aqueous layer was separated and analyzed for total solids, ash, lactose, protein, calcium, phosphates, and sodium content along with color. MFT did not influence the analyzed whey components ( $P > 0.05$ ) except for lactose. However, addition of sepiolite influenced protein content and  $a^*$  and  $b^*$  color values for the top aqueous layers ( $P < 0.05$ ). Both levels of sepiolite addition resulted in about a 50% decrease in protein compared to original GYW. Adding two grams of Sepiolite per 100g of GYW from manufacturer 1 resulted in  $b^*$  decreasing from 25.99 to 8.16 compared to treated GYW with no

sepiolite. Sepiolite was found to have possible applications in the removal of proteins and color pigments in GYW.

# Table of Contents

List of Figures .....	vii
List of Tables .....	viii
Acknowledgements .....	ix
Dedication .....	x
Chapter 1 - Literature Review .....	1
Introduction .....	1
Dairy Consumption and Waste Production .....	1
Greek Yogurt Whey .....	3
Importance of Calcium .....	5
Greek Yogurt Whey Processing Challenges .....	6
Possible Treatment Method – 1: Sepiolite Clay Addition .....	7
Introduction into Sepiolite Properties and Uses .....	7
Sepiolite as an Adsorbent for Heavy Metals .....	8
Sepiolite as an Adsorbent for Dye Pigments .....	9
Removal of Proteins using Sepiolite .....	11
Sepiolite as a Clay-Modified Electrode .....	11
Conclusions on Sepiolite as a Feasible Physical Treatment .....	13
Possible Treatment Method – 2: Magnetic Fluid Treatment .....	13
History behind Magnetic Fluid Treatment .....	13
Fluid Types Treated with Magnetic Fluid Treatment .....	14
Development of Magnetic Fluid Treatment Systems and Parameters .....	16
Methods for Evaluating the Effectiveness of Magnetic Fluid Treatment .....	20
Proposed Magnetic Fluid Treatment Mechanisms .....	25
Conclusions on Magnetic Fluid Treatment as a Feasible Physical Treatment .....	28
Conclusion .....	29
Tables .....	30
References .....	33
Chapter 2 - Research Objectives .....	37

Chapter 3 - Magnetic Fluid Treatment and Sepiolite Addition as Methods for Concentrating	
Greek Yogurt Whey Components .....	38
Abstract.....	38
Introduction.....	40
Materials and Methods.....	43
Experimental Design.....	43
MFT System Development.....	43
Sepiolite .....	44
Process Description: MFT and Sepiolite Addition .....	44
Chemical and Physical Analysis.....	45
Identification of Proteins on the Sepiolite Surface .....	47
Scanning Electron Microscopy (SEM).....	47
Statistical Analysis.....	48
Results and Discussion .....	49
Modeling of MFT Chamber.....	49
Greek Yogurt Whey.....	49
Effect of Magnetic Field on GYW Components .....	49
Effect of Sepiolite Addition .....	51
Conclusions.....	59
Acknowledgements for Chapter 3 .....	60
Figures .....	60
Tables.....	66
References.....	69
Appendix A - Image of Magnetic Fluid Treatment System from Chapter 3 .....	71
Appendix B - Additional Theoretical Magnetic Field Design for Chapter 3 .....	72
Appendix C - Raw Data and SAS Code for Manufacturer 1 for Chapter 3.....	73
Appendix D - Raw Data and SAS Code for Manufacturer 2 for Chapter 3 .....	79
Appendix E - Additional SEM Images for Chapter 3.....	85
Appendix F - Images of Color Change in Greek Yogurt Whey Top Aqueous Layers from Sepiolite Addition for Chapter 3.....	95

## List of Figures

Figure 3.1 Magnetic Fluid Treatment system design.....	60
Figure 3.2 Process flow diagram for treatment of Greek yogurt whey .....	61
Figure 3.3 Theoretical magnetic flux density plot for the Magnetic Fluid Treatment chamber...	62
Figure 3.4 SEM image of sepiolite .....	63
Figure 3.5 SEM image of sepiolite with GYW.....	64
Figure 3.6 Confocal microscopy image of dyed whey proteins on sepiolite surface (a) with corresponding SEM image (b) where green indicates the presence of proteins on the surface .....	65

## List of Tables

Table 1.1 Greek yogurt whey compositional analysis (U.S. Dairy Export Council, Arlington, VA, personal communication).....	30
Table 1.2 Summary of magnetic water treatment studies using permanent magnets.....	31
Table 1.3 Summary of magnetic water treatment studies using electric magnets.....	32
Table 3.1 Chemical composition of Greek yogurt whey collected from manufacturer 1 and manufacturer 2 (mean $\pm$ standard deviation; n=2).....	66
Table 3.2 Effect of magnetic exposure and addition of sepiolite to the chemical composition of the top aqueous layers of Greek yogurt whey (mean $\pm$ standard deviation; n=2).....	67
Table 3.3 X-ray elemental component analysis.....	68



## **Acknowledgements**

Thanks to everyone that supported me, gave me guidance, or aided in my research throughout my graduate career. Especially, my family and friends, Food Science Institute professors and staff, my lab mates, and all other Kansas State University departments that helped me in developing or analyzing my research.

## **Dedication**

My Master's work is dedicated to my parents, Kay and Darel Kyle, and my sister Laraine Cory that have supported me throughout my entire time at Kansas State University.

# **Chapter 1 - Literature Review**

## **Introduction**

Greek yogurt is produced by removing water and water soluble components, Greek yogurt whey (GYW), from yogurt. GYW's chemical properties including high mineral content, low pH, and relatively low concentrations of valuable components like proteins and lactose make it difficult to economically process with traditional processing methods. Table 1.1 contains the average chemical composition of GYW. For example, GYW contains high amounts of lactic acid and galactose that are hygroscopic and hinder drying processes (Keller, 2015). This issue has become more relevant recently in the United States with the increased popularity of Greek yogurt. The purpose of a successful GYW treatment method is to isolate valuable components including lactose, minerals, and protein to make value-added processes or sewage treatment more economical. The purpose of this literature review is to focus on problems associated with GYW while reviewing the use of and mechanisms behind possible physical treatment methods for GYW including magnetic fluid treatment and the addition of a clay mineral, sepiolite.

## **Dairy Consumption and Waste Production**

Large volumes of nutrient-dense waste-streams result as the dairy industry accommodates for an increased consumer demand for dairy products. For example, the number of milk-producing bovines in the world in 2007 was estimated to be 125 million and the world's production of cow's milk was projected to be 427,585 million kilograms. Cheese production in the United States was estimated at 4,412 million kilograms for 2007 as well (Chandan et al., 2009). Yogurt production in the United States was around two billion kilograms in 2009 with the American per capita consumption of yogurt increasing 400% from 1982 to 2012 (Desai et al., 2013). The production scale necessary to meet consumer demands around the world causes the

production of large amounts of waste. For example, cheese manufacturing typically involves the production of nine liters of whey for every kilogram of cheese produced. About 160 million metric tons of whey are produced annually in the world with about a 1 - 2% annual growth rate, where half of the whey produced is discarded as waste (Kosseva and Webb, 2013). According to Kosseva and Webb (2013), a dairy facility that produces 100 metric tons of milk per day produces approximately the same amount of organic products in their waste streams as a town with 55,000 residents. The dairy industry has multiple sources of waste creation while the components of the waste itself cause problems with proper disposal.

According to Sarkar et al. (2006), dairy waste-streams are distinguished by high biochemical and chemical oxygen demand contents, and high levels of suspended solids including fats, ammonia, or minerals. Therefore, dairy waste-streams require appropriate treatment before disposal. Besides the dairy products themselves, some of these components stem from detergents and sanitizers from cleaning processes (Kosseva and Webb, 2013). The organic components in the effluent include high concentrations of whey proteins, minerals, fat, and lactose (Sarkar et al., 2006). Waste composition varies notably among processing days, dairy products, and dairy plants. The biochemical oxygen demand varies from 40 -  $48 \times 10^3$  mg/L while the chemical oxygen demand varies from 80 -  $95 \times 10^3$  mg/L. The pH ranges from 4.7 - 11 and the amount of suspended solids ranges from 0.024 - 4.5g/L. The nitrogen and phosphorus contents are typically around 14 - 830mg/L and 9 - 280mg/L respectively. Nitrogen from dairy proteins is present in organic form as urea, nucleic acids, or protein or in ionic form as  $\text{NH}_4^+$ ,  $\text{NO}_3^-$ , or  $\text{NO}_2^-$ . Phosphorus is commonly found in its inorganic forms including polyphosphate and orthophosphate. Other ions including Cl, K, Ca, Na, Mn, Ni, CO, Mg, and Fe are also present

(Kosseva and Webb, 2013). Composition and characteristics of common dairy waste-streams are given by Demirel et al. (2005).

The properties of dairy plant effluents including varying pH conditions, nutrient-rich components, and the presence of cleaners or detergents make its disposal a challenge. The treatment of waste-water from dairy plants involves multiple physical, chemical, or biological treatments to produce water able to be recycled and unwanted collected sludge that could be disposed of. The layout, equipment, and processes chosen depend on the capabilities and demands of the dairy plant (Bylund 2003).

### **Greek Yogurt Whey**

Nsabimana et al. (2005) defined *labneh* as “a concentrated yogurt widely produced and consumed in the Middle Eastern countries and Balkans.” This semisolid food is derived by straining or filtering yogurt to achieve a product with higher fat and protein content, creamy white color, smooth texture, and an acidic flavor. Similar products to *labneh* are produced elsewhere including Egypt, Turkey, Bulgaria, Iceland, India, and the United States (Nsabimana et al., 2005).

Traditional *labneh* preparation involves straining yogurt through cloth, animal skin, or porous ceramic material until the desired total solids content is achieved. Modern industrial methods to produce *labneh* include membrane filtration techniques and centrifugation (Nsabimana et al., 2005).

The United States has a strained yogurt product very similar to *labneh* referred to as Greek yogurt or concentrated yogurt. Greek yogurt is also produced by removing water and water soluble components from yogurt. The United States does not currently have a standard of identity for Greek yogurt (Desai et al., 2013). American consumer demand for Greek yogurt is

steadily rising. Greek yogurt sales in the United States rose from \$33 million in 2007 to \$469 million in 2010 accounting for 12% of all yogurt sales (Schultz and Parekh, 2011). Recently, Greek yogurt is estimated to account for more than 25% of yogurt sales in the United States (Desai et al., 2013). It is necessary for United States Greek yogurt manufactures to properly dispose of or find additional value for the water and water soluble components, Greek yogurt whey (GYW), resulting from this increase in Greek yogurt demand.

According to Wail-Alomari et al. (2011), whey from *labneh* is typically composed of about 94% water, 0.4% fat, 0.8% ash, 4.9% lactose, and 0.75% protein, and has a pH close to 4.5. The reported values, especially for protein and lactose, from Wail-Alomari et al. (2011) vary from values recorded for GYW. In the United States, GYW on average has the following composition 4.45 pH, 5.77% total solids (TS), 0.72% ash, and 3.53% lactose. Table 1.1 contains detailed compositional analysis for GYW collected from ten United States Greek Yogurt manufacturing sites (U.S. Dairy Export Council, Arlington, VA, personal communication). For comparison, cottage cheese whey typically has the following characteristics 6.4% TS, 0.75% ash, 4.6% lactose, 0.7% total protein, and pH of 4.5 (Chandan and Kilara, 2010). Sweet whey from cheese making has a pH around 5.9 and the following average chemical properties 6.4% TS, 0.85% total protein, 5.0% lactose, and 0.65% ash (Chandan and Kilara, 2010). GYW tends to have less valuable components including lactose and protein compared to whey from cheese or cottage cheese manufacturing.

In the Jordanian food industry about 99% of the whey from *labneh* production is disposed of in the sewage system causing a high biochemical oxygen demand and other environmental concerns (Wail-Alomari et al., 2012). Products derived from *labneh* whey have been utilized in bakery products including crackers and French bread, sweet lactose syrup, and during other dairy

products production, including cheese and sour cream, to make use of the nutritional components and limit environmental waste (Alsaed et al., 2013). Therefore, there could be opportunities to add value to GYW as well.

### **Importance of Calcium**

Calcium is an important mineral for the health of living creatures (Haug et al., 2007). About 99% of the calcium stores in the human body are inside bones and teeth. Calcium in bones provides strength to the skeletal system and acts as a reservoir to properly maintain extracellular calcium levels. Obtaining proper calcium levels in bones is vital for children because over 90% of a person's bone mass is achieved before the age of twenty. Besides bone health, calcium is a secondary messenger for transmitting signals within plasma membranes and is a cofactor in clotting mechanisms. Low dietary calcium intake has been linked to increased risk of hypertension, colon cancer, osteoporosis, and premenstrual syndrome (Power et al., 1999). Dairy products are an excellent source of dietary calcium because bovine milk contains on average one gram of calcium per liter of milk. In addition, dairy products provide over half of the calcium intake in the average American diet (Haug et al., 2007).

Calcium is also vital for animal health. Improper calcium intake can cause milk fever and ketosis for bovines (Goff, 2006). Swine diets high in calcium cause the meat to be tenderer by increasing the activity of proteases, specifically calpains (Pettigrew and Esnaola, 2001). In the animal industry calcium helps to improve the quality of animal products and preserve the health of the animals themselves.

Heat and pH adjustment can be utilized to recover calcium from different sources including dairy waste-streams. GEA Filtration (Hudson, WI) developed parameters to precipitate calcium phosphate from whey ultra filtrate and found that calcium phosphate is less soluble with

increasing pH and increasing temperature. Heating the pre-concentrated whey to 75 - 80°C and adjusting the pH to 6.9 - 7.2 resulted in the highest amounts of precipitated calcium phosphate. High pH levels favor the formation of insoluble tricalcium phosphate from soluble monocalcium phosphate (Corredig, 2009). Whey proteins, lactose, and most other whey constituents remain stable with increased pH. However, the addition of bases can cause lactic acid salts to form. For example, sodium hydroxide reacts with lactic acid to form sodium lactate. At 75°C calcium hydroxyphosphate loses water and forms insoluble calcium orthophosphate. Temperatures above 65°C cause whey proteins to start denaturing, but lactose does not experience browning reactions until temperatures reach 100°C (Bylund, 2003). Chemical properties of whey can be manipulated to favor the precipitation of calcium.

### **Greek Yogurt Whey Processing Challenges**

With an acidic pH around 4.45 pH and a relatively high ash content of about 0.72%, GYW creates issues with pipe and equipment scaling, and GYW's relatively low protein and lactose content make it less valuable compared to sweet whey (U.S. Dairy Export Council, Arlington, VA, personal communication). In addition, GYW cannot be readily processed with traditional drying methods because it contains a relatively high amount of hygroscopic components, including lactic acid and galactose. GYW also contains small amounts of components that aid in drying processes, including high-molecular-weight proteins and lactose monohydrate (Keller, 2015). Therefore, nontraditional methods besides evaporation and filtration are necessary to economically process GYW. Possible processing methods for the GYW include land application, bioreactors, and animal feed. The application of GYW to fields is limited due to concerns about impact to soil quality caused by the GYW's high acidity and mineral content. GYW does not have enough nutrients to be a primary component of animal feed. Both land



application and animal feed utilization incur costs related to transporting the GYW from the dairy processing plant to the farm. Bioconversion has the potential for breaking down the nutritional components in GYW but requires consistent nitrogen and carbon sources. A method capable of extracting or concentrating the lactose, minerals, and protein would be the best solution for treating or gathering value from GYW (U.S. Dairy Export Council, Arlington, VA, personal communication).

## **Possible Treatment Method – 1: Sepiolite Clay Addition**

### ***Introduction into Sepiolite Properties and Uses***

Guney et al. (2014) describes sepiolite as “a natural clay mineral ( $\text{Mg}_4\text{SiO}_6\text{O}_{15}(\text{OH})_2 \cdot 6\text{H}_2\text{O}$ ) with fibrous morphology and intracrystalline channels.” Alternating blocks and tunnels form the general structure of this specific magnesium silicate compound (Doğan et al., 2007). According to Doğan et al. (2007), each block consists of two tetrahedral silica sheets enclosing a central octahedral magnesia sheet where the silica sheets are discontinued and inversion of these sheets give rise to structural channels. Sepiolite’s molecular-sized channels are responsible for its high specific surface area and high surface activity which allow for heavy metals to be easily attached and retained (Guney et al., 2014). Other desirable properties of sepiolite include high mechanical and chemical stability, abundant supply, and the ability to adsorb both organic and inorganic ions. Sepiolite is commonly used in the production of paint, paper, cosmetics, and detergents and in the treatment of waste-streams (Doğan et al., 2007). Sepiolite is also used as a feed additive for all animal species acting as a binder and anti-caking agent (Parisini, 1999). The many desirable properties of sepiolite led to studies exploring its uses in industrial waste treatment applications, as a dye or protein adsorbent, and as part of electrochemical sensors.

### *Sepiolite as an Adsorbent for Heavy Metals*

In industrial waste treatment sepiolite is a material option for waste-stream filters and bottom liners for solid waste sites because of its absorbent properties, especially with heavy metal ions. Brigatti et al. (1999) passed a model metal ion solution at a rate of 0.29mL/s through a chromatographic column packed with 50g of sepiolite with 580nm diameter pores. The model solution contained  $\text{Co}^{2+}$ ,  $\text{Cu}^{2+}$ ,  $\text{Zn}^{2+}$ ,  $\text{Cd}^{2+}$ , and  $\text{Pb}^{2+}$  ions in distilled water. Each cation in the solution had a concentration of  $2 \times 10^{-3}\text{N}$ . A  $2 \times 10^{-3}\text{N}$  sodium solution was used to regenerate the column in order to observe the column's ability for reuse. The researchers evaluated sepiolite's effectiveness as an adsorbent for removing waste-water pollutants based on its adsorption and desorption properties. All effluent samples were analyzed using atomic absorption and inductively-coupled plasma to determine ion concentration (Brigatti et al., 1999).

According to Brigatti et al. (1999), total amount of cations retained and eluted by the beds was determined by integrating areas above the breakthrough and below elution curves. In the sepiolite column, 0.017mequ/g  $\text{Co}^{2+}$ , 0.034 mequ/g  $\text{Cu}^{2+}$ , 0.029 mequ/g  $\text{Zn}^{2+}$ , 0.022 mequ/g  $\text{Cd}^{2+}$  and 0.017 mequ/g  $\text{Pb}^{+}$  were retained. After elution with the sodium solution some of the ions on the column were still retained including about 17.6%  $\text{Co}^{2+}$ , 88.2%  $\text{Cu}^{2+}$ , 65.5%  $\text{Zn}^{2+}$ , 40.9%  $\text{Cd}^{2+}$  and 17.6%  $\text{Pb}^{+}$ . Lead and cobalt were the least retained after the column was regenerated. Copper and zinc had the highest affinity for sepiolite while lead and cobalt had the lowest. According to the elution curve for the sepiolite column, magnesium and calcium were initially released readily and the total eluted for each ion was 0.100meq/g and 0.070meq/g, respectively. The absorbent properties of sepiolite for specific metal ions described by this study can be considered when choosing a material for waste-stream treatment (Brigatti et al., 1999).

Guney et al. (2014) examined the potential of soil mixtures composed of sepiolite and another silicate mineral, a zeolite composed of 81.1% SiO<sub>2</sub>, 12.5% Al<sub>2</sub>O<sub>3</sub>, and 2.7% CaO, as bottom liners for landfills. Batch adsorption studies were conducted by mixing 7g of the sepiolite/zeolite mixture with 75ml of a metal solution for 3h, centrifuging the resulting mixture at 150rpm for 24h, and then filtering the sample for mineral analysis using atomic absorption spectroscopy. The following metal solutions were used copper (II) chloride (200mg/L), Zinc chloride (200mg/L), CrCl<sub>3</sub>·6H<sub>2</sub>O (2,000mg/L), lead (II) chloride (1,000mg/L), and FeCl<sub>3</sub>·6H<sub>2</sub>O (3,000mg/L). The concentration of lead, copper, and zinc cations in the eluent from the column decreased as the ratio of sepiolite to zeolite increased. The ion retention for each column type was given by Guney et al. (2014). Sepiolite has about three times the surface area of zeolite which could be the cause of the higher metal ion retention in sepiolite-rich mixtures. Retention of the metal ions increased with increasing pH of the effluent. Increasing the amount of sepiolite in the mixture did not influence the pH of the effluent solutions. This recent study helped to confirm the waste treatment potential of sepiolite (Guney et al., 2014).

### ***Sepiolite as an Adsorbent for Dye Pigments***

The adsorption properties from the high surface area of sepiolite have applications in the removal of dye components. Types of dyes that could be adsorbed by sepiolite and the mechanism that determined the rate of adsorption were examined. The general approach to each study was to mix sepiolite with a dye solution and determine the amount of dye that was retained under certain conditions, including ionic strength, pH, and temperature (Doğan et al., 2007). Özcan et al. (2006) observed that when adsorbing an acid dye, Acid Blue 193, with sepiolite the adsorption was dependent on pH, contact time, and temperature. Increasing temperatures led to less dye being removed by sepiolite. Doğan et al. (2007) treated solutions containing methyl

violet and methylene blue with sepiolite, and discovered that the adsorption rate of these dyes by sepiolite increased with an increase in initial dye concentration, pH, ionic strength, and temperature. However, stirring speed was not an important factor. Tekbaş et al. (2009) observed that the adsorption of Basic Astrazon yellow 7GL by sepiolite was endothermic in nature. The mechanism for adsorption of all of the dyes in each study by sepiolite was described using pseudo-second order kinetic reaction models (Tekbaş et al., 2009). Sepiolite has proven to be an effective adsorbent of dye pigments.

Clay minerals could have applications in removing color from dairy products. For example, Kang et al. (2012) looked at alternative methods for removing annatto colorant, norbixin, from cheese whey. One of the methods involved adding acid-activated bentonite to cheese whey prepared with 3% w/v norbixin. The acid-activated bentonite was prepared by mixing 20g of bentonite with 2N sulfuric acid, heating the mixture to 90°C for 4h, and rinsing the mixture with distilled water until a pH of 4 was reached. Acid-activated bentonite powder was added to the liquid cheese whey (0.5% w/v) and recirculated at 50°C for 60min. The solution was then centrifuged for 10min at 8,000g and the residual norbixin was measured. About 79% of the norbixin in the cheese whey was removed by the acid-activated bentonite treatment. The dye adsorption was contributed to norbixin adsorbing into interlayer sites in the acid-activated bentonite (Kang et al. 2012). In addition, sepiolite has shown to have applications in bleaching cheese whey. Adding about 2% of sepiolite to cheese whey resulted in over a 30% color reduction (J. Amamcharla, unpublished data). Therefore, sepiolite could have applications in color removal for GYW.

### ***Removal of Proteins using Sepiolite***

Sepiolite could have the potential to remove proteins from aqueous solutions. According to Yu et al. (2013), clay minerals can interact with proteins using any of the following mechanisms cation exchange, cation bridge, hydrogen bonding, hydrophobic interactions, hydrophilic interactions, van der Waals forces, and electrostatic interactions. Barral et al. (2008) used kaolinite, a layered aluminosilicate clay mineral, to adsorb bovine serum albumin (BSA), beta-lactoglobulin ( $\beta$ -LG), and alpha-lactalbumin ( $\alpha$ -LA) from whey protein solutions. Maximum adsorption capacity was reached at the isoelectric point for each whey protein. Kaolinite adsorbed 131mg of  $\alpha$ -LA, 52mg of BSA, and 77.5mg of  $\beta$ -LG per gram of kaolinite. X-ray diffraction analysis determined that protein adsorption takes place on kaolinite's external edges and surfaces. A lack of hydrogen bonding between whey proteins and the hydroxyl groups onto the surface of kaolinite's was confirmed using Fourier transform infrared spectroscopy. Barral et al. (2008) concluded that electrostatic interactions were the primary mechanism behind protein adsorption onto kaolinite surfaces. In addition, steric effects might also play a minor role. Similarly, sepiolite added at 1% to cheese whey was shown in a separate study to remove up to 40% of the whey proteins (J. Amamcharla, unpublished data). The ability of sepiolite to remove whey proteins could help to isolate whey proteins from other GYW components.

### ***Sepiolite as a Clay-Modified Electrode***

The adsorption properties of sepiolite allow it to have applications as a sensor for certain analytes. Clay-modified electrodes have applications for the development of electrochemical and biological sensors to detect various analytes ranging from cationic species, such as metal cations, and organic molecules, including water pollutants to products of enzymatic reactions (Mousty, 2004). According to Mousty (2004), most clay-modified electrodes were prepared using covalent

bonding, chemisorption, and film deposition. The ability to preconcentrate an analyte, natural electrocatalytic properties, and the capacity to immobilize reagents are all desirable properties for clay minerals used as part of clay-modified electrodes. Studies focused on using clay-electrodes prepared with sepiolite to detect various chemical analytes including clozapine (limit of detection (LoD) =  $1 \times 10^{-7} \text{M}$ ), dinocap (LoD =  $8 \times 10^{-10} \text{M}$ ), aniline (LoD =  $1.6 \times 10^{-7} \text{M}$ ), phenol (LoD =  $3.2 \times 10^{-7} \text{M}$ ), ephedrine (LoD =  $1.8 \times 10^{-5} \text{M}$ ), linuron (LoD =  $3.0 \times 10^{-7} \text{M}$ ), bentazepam, nitrobenzene (LoD =  $1.6 \times 10^{-6} \text{M}$ ), tetramethrin (LoD =  $1.4 \times 10^{-7} \text{M}$ ), and 2-sec-butyl-4, 6-dinitrophenol (Mousty, 2004). Sepiolite has the potential for aiding in detection of chemical analytes.

Esteban-Cubillo et al. (2007) developed a humidity sensor using iron-oxide nanoparticles and sepiolite. Sepiolite was chosen as the supporting matrix for the sensing component, iron-oxide, because of its high surface area and open pores. A high surface area was needed to support the iron-oxide while improving the sensibility. Open pores were vital for proper gas and water adsorption and condensation. Depending on the hematite content, the humidity sensors had a relative humidity detection range of 5 - 98% while exhibiting a low production cost (Esteban-Cubillo et al., 2007).

Erdem et al. (2012) used sepiolite as a supportive matrix for a DNA electrochemical detector electrode. The sepiolite channels allowed for ion penetration and adsorption areas for molecules. The channels combined with sepiolite's high surface area resulted in desirable catalytic and adsorptive properties. Sepiolite provided a 1.95-fold higher guanine signal and 6.25-fold higher adenine signal (Erdem et al., 2012). The enhancing effect was contributed to sepiolite's higher surface area for the modification of nucleic acid (Erdem et al., 2012).

## ***Conclusions on Sepiolite as a Feasible Physical Treatment***

Sepiolite has desirable physical characteristics that can be applied in the industry, especially with waste treatment. Most studies regarding sepiolite focused on its ability to remove heavy metal ions or dyes from waste-streams. There is a need for studies that highlight the use of sepiolite in other industries or as a method of adding value to food products. One example of adding value could be extracting minerals or proteins from food waste-streams or removing unwanted pigments.

## **Possible Treatment Method – 2: Magnetic Fluid Treatment**

### ***History behind Magnetic Fluid Treatment***

Calcium carbonate precipitates in hard water, which is water with high calcium and magnesium ion content, by displacing the equilibrium of the calcoarbonic system:

$$\text{Ca}^{2+} + 2\text{HCO}_3^- \rightleftharpoons \text{CaCO}_3(\text{s}) + \text{CO}_2 + \text{H}_2\text{O} \text{ (Alimi et al. 2009).}$$

Calcium carbonate deposits can cause harm to water systems and piping that use hard or natural water in domestic, industrial, and agricultural applications (Strazisar et al., 2001). The detrimental effects range from clogging membranes and pipes to decreasing the efficiency of water heating systems (Alimi et al., 2009). Because calcium carbonate is less soluble at higher temperatures, the hard scale or calcium carbonate precipitate is the most damaging to hot-water systems including boilers and heat exchangers (Coey and Cass, 2000). The chemical methods used to reduce water scaling, including the addition of lime or ion exchange systems, can be effective but are not cost effective and change the water chemistry significantly, sometimes resulting in harmful health effects if the water is consumed (Lipus and Dobersek, 2007). A physical treatment like magnetic fluid treatment that does not involve chemical reactants or harming the potability of the water can be a better method for hard water scale reduction

Magnetic water treatment systems are not a new concept. The first commercial magnetic water treatment device was patented in 1945 in Belgium while magnetic water treatment systems have been used in America since 1975. Reported claims for the treatment include lower scale formation rate, development of soft scale formations, change in size of precipitated particles, increased ratios of aragonite, and change in the nucleation rate of calcium carbonate. No significant effects also have been reported (Strazisar et al., 2001).

Claims about the effectiveness of the treatment on hard water scaling have been controversial for over 50 years (Cai et al., 2009). The main reasons for the controversy focus on both laboratory and industrial studies having low reproducibility, the existence of reports with conflicting results, and the lack of an accepted and proven mechanism explaining how the magnetic field alters the water's properties (Busch and Busch, 1997). Consequently, scientific literature comparing experimental parameters, analytical testing methods, and proposed mechanisms of magnetic water treatment studies was reviewed. In this portion of the review, the aim is to shed light on those conclusions and results regarding the treatment that would be reproducible and agreed upon in the scientific community. The food industry relies on water systems for processing and cleaning. Therefore, food processing plants can benefit from safe methods designed to reduce hard water scaling. The concept of using magnetic fluid treatment to alter the properties of minerals in primarily water solutions could also be related to food waste-stream treatment and certain food processing procedures.

### ***Fluid Types Treated with Magnetic Fluid Treatment***

A majority of magnetic fluid treatment studies mostly focus on treating water samples because of the economical impact of hard water scaling. The water samples used within the studies include hard water from natural sources, purified water, and model electrolyte solutions.



Coey and Cass (2000) individually drew groundwater from a limestone well and commercial mineral water through a static magnetic field using gravity. A significant change in the calcium carbonate properties from magnetic treatment was observed at a 99.9% probability level for both water samples. Another study by Cai et al. (2009) featured pumping purified water through a static magnetic field to observe the magnetic field's effect on the water's hydrogen bonding properties. Observations including a decrease in surface tension and an increase in viscosity with magnetic treatment were used to support the hypothesis that the magnetic field increases the average water cluster size. A water purification system was used to purify the water source so that the water used in the experiments had specific properties including organic carbon concentration below 0.05mg/L, dissolved oxygen concentration below 5.0mg/L, and a resistivity of around 18.2M $\Omega$  at 25°C.

Knez and Pohar (2005) dissolved analytical grade calcium carbonate in deionized water by pumping carbon dioxide gas through the suspension for two days until the final concentration of calcium carbonate in the solution was between 1.000 -1.200g/L. The solution was pressure filtered through 0.04 $\mu$ m pores to remove solid particles. Changes were observed in the properties of the dissolved calcium carbonate, an increase in the amount of aragonite, after passing the solution through an electromagnetic chamber (Knez and Pohar, 2005).

A separate study prepared electrolyte solutions using analytical grade inorganic salts including sodium chloride, potassium chloride, sodium phosphate, and calcium chloride. The salts were dissolved in double distilled water and the resulting solution was then deionized. The electrolyte solutions were sealed inside a magnetic chamber for various amounts of time. A change in conductivity of the electrolyte solutions was observed (Holysz et al., 2007). Magnetic water treatment studies are not consistent with the water source or the solution composition and

preparation, but most of them claim to have notable observations. Such variety among the experimental samples can make comparing results from different studies difficult. Most of the experimental samples did not represent industrial situations which would make applying any results to industrial processing systems difficult.

### ***Development of Magnetic Fluid Treatment Systems and Parameters***

Researchers typically agreed that the experimental parameters played a vital part in the effectiveness of magnetic treatment of water. However, uncertainty existed on which parameters are the most important and the exact experimental conditions. This causes a lack of consistency among the experimental apparatuses and designs among magnetic treatment of water studies. The main experimental factors that could have the most influence include type of magnet being used, magnetic field strength, magnetic exposure time, flow rate of the sample, orientation of the magnetic field, and pipe or container material (Holysz et al., 2007).

Permanent magnets are the most popular type of magnets when designing magnetic treatment devices because of their lower operational costs compared to electromagnets. Ambashta and Sillanpää (2010) mentioned that “permanent magnets have been prepared from ferromagnets of iron-based, nickel-based, cobalt-based or rare earth element-based compounds.” Advancements in materials and processing have made it possible to increase the magnetic field strength of permanent magnets from less than one Tesla to about two Tesla if multiple magnets are used (Ambashta and Sillanpää, 2010). Most studies arrange multiple permanent magnets to produce a magnetic field less than one Tesla despite the ability to create a stronger field (Botello-Zubiate et al., 2003). According to Kobe et al. (2002), successful treatment requires a magnetic field of at least 0.5 Tesla. However, studies with magnetic fields lower than 0.5 Tesla still claimed reduction in hard water scale (Fathi et al., 2006). According to published reports, the

amount of time the water was exposed to a magnetic field produced by permanent magnets varied from a few minutes to over 60min (Li et al., 2007). The permanent magnetic studies almost equally represent designs featuring the sample moving through the magnetic field or being stagnant while exposed to the magnetic field (Holysz et al., 2007). The permanent magnet water treatment systems vary greatly in design but they generally involve arranging multiple magnets especially in an alternating fashion (Fathi et al., 2006).

Fathi et al. (2006) designed a permanent magnet apparatus to observe calcium carbonate scale formation of hard water under a magnetic field. A loop of 1.50m of clear polyvinyl chloride tubing with a cross section of  $0.38\text{cm}^2$  was connected to a closed glass tank. A volumetric gear pump was attached to the circuit and adjusted to pump 0.5L of water with a moderate flow rate in the laminar region with Reynolds number below 2,040 through the system. According to Fathi et al. (2006), the magnetic device consisted of five pairs of permanent magnets associated alternately with north and south faces facing each other. Each magnet pair was closed with an iron token. The resulting field strength of the magnetic device that the sample was exposed to was about 0.16 Tesla. This design allowed for the sample to be pumped through the system, avoided notable contamination from pipe and container materials, and arranged the magnets in a simple manner.

According to Ambashta and Sillanpää (2010), electromagnets are solenoids of electrical conducting wires that generate adjustable magnetic fields up to 2.4 Tesla when electric current passes through the wires. Even though electromagnets are capable of higher ranges than permanent magnets, magnetic water treatment studies that involved electromagnets normally used magnetic fields with field strengths of one Tesla or lower. Pumping the sample was the

most popular option with electromagnetic water treatment systems, and the sample was typically circulated through the system for less than ten minutes.

Cho and Lee (2005) compared a permanent and an electromagnet system to observe which device best lowers the surface tension of hard water. The researchers observed a drop in the surface tension of the hard water when treated with either system. Their observations suggest that whether the magnetic field was produced using permanent or electromagnets, effectiveness of the magnetic fluid treatment should be the same. Even though electromagnet systems have higher operational costs than permanent magnet systems, electromagnets can have more adjustable and higher field strengths.

Knez and Pohar (2005) used an electromagnetic device with calcium carbonate electrolyte solutions to observe magnetic field effects on calcium carbonate structure. A recirculating system was constructed using 3m of silicon tubing with an inner diameter of 0.7cm attached to a peristaltic pump and a one liter glass container. The pump produced flow rates from 0.1 to 3.0L/min. The electromagnet had adjustable magnetic flux densities based on the direct electric current strength and the adjustable gap between the magnetic poles. An AC/DC transformer supplied the current, and the sample was designed to flow orthogonally with respect to the magnetic field. The major advantages of this system were the ability to easily adjust the flow rate and magnetic field properties (Kenz and Pohar, 2005).

The rate at which the sample flowed through the magnetic field or whether the sample was moving through the field at all could be important design aspects for magnetic water treatment systems. Kobe et al. (2002) claims that the fluid must pass orthogonally with respect to the magnetic field at velocities of 0.5 - 2.0m/s with Reynolds numbers in turbulent region above 2,040 in order to observe measurable effects from magnetic treatment. Strazisar et al. (2001)

performed static magnetic treatment, sample stagnant during magnetic exposure, and dynamic magnetic treatment, sample moving through the magnetic field, with calcium carbonate solutions. Dynamic and static magnetic treated solutions both had higher amounts of calcium carbonate in aragonite form compared to solutions that did not receive magnetic fluid treatment. These results suggest that both methods can be effective and contradict the hypothesis that only dynamic magnetic fluid treatment was effective (Strazisar et al., 2001).

Alimi et al. (2009) treated calcium carbonate solutions by passing them through a series of permanent magnets at flow rates within the laminar region with Reynolds number below 2,040. The magnetic fluid treatment appeared to have increased the amount of calcium carbonate precipitated compared to no magnetic fluid treatment. Their observations of the formed calcium carbonate crystals contests the theory that the flow rate must be in the turbulent region in order for the magnetic fluid treatment to be effective (Alimi et al., 2009). Another experiment passed calcium carbonate solutions through a series of permanent magnets at various flow rates ranging from 0.5 - 0.94 L/min. Higher crystal nucleation in the bulk solution was observed as the flow rate increased. Almost all studies prefer that the fluid flows orthogonally in relation to the magnetic field. However, no explanation was given for selecting this flow direction (Alimi et al., 2007). The choice to move the sample through the magnetic field or not has not been proven to be a major factor for obtaining successful magnetic fluid treatment.

The chemical and physical properties of the surfaces that the water or sample comes into contact with has been shown to not greatly influence or hinder the effects of magnetic fluid treatment. However, the surface material has been shown to be a factor in the amount of hard scale formation on the surface. Alimi et al. (2009) suggested that a combination of the surface material and magnetic fluid treatment led to a notable reduction in hard scale formation. Alimi et

al. (2009) pumped calcium carbonate solutions at flow rates of 0.54L/min, 0.74L/min, and 0.94L/min, through a permanent magnetic device with field strength of 0.16 Tesla with the following pipe materials polytetrafluoroethylene (PTFE), Tygon, polyvinyl chloride (PVC), copper, and stainless steel. The study concluded that magnetic water treatment caused notably more calcium carbonate formation in the bulk solutions rather than on the surfaces. However, the pipe material that was used was not an important factor. Other conclusions included that the magnetic field effect was lower for conductive materials, rougher materials have less hard scale formation, and PTFE had the most hard scale formation while Tygon had the least (Alimi et al., 2009). The hard water scale formation from magnetic fluid treatment for each pipe material that was examined was given by Alimi et al. (2009).

Chibowski et al. (2003) dipped aluminum, glass, copper, and steel surfaces in stagnant calcium carbonate solutions for two hours with and without the presence of a 0.1 Tesla permanent magnetic field at various temperatures. Aluminum had the least amount of calcium carbonate deposits on the surface while stainless steel had the most. The researchers claimed that the magnetic fluid treatment caused nearly a 40% reduction in the calcium carbonate deposits depending on the surface and temperature (Chibowski et al., 2003). Contact surface material was not a major factor for the effectiveness of the magnetic fluid treatment but could influence the overall hard water scale.

### ***Methods for Evaluating the Effectiveness of Magnetic Fluid Treatment***

In the studies on magnetic fluid treatment, various methods have been used to determine if the hard water scaling was reduced or if the water's properties were changed. Observing and measuring the amount of precipitate that forms was the simplest experimental method that related directly to the goal of reducing mineral build-up. Lipus and Dobersek (2007) studied

magnetic water treatment by pumping tap water through two hot water heaters at a rate of 0.2L/min for three weeks. The inlet pipe to one boiler contained permanent neodymium magnets with an alternating arrangement on the outside resulting in a 0.1s water retention time. Segments of the piping and heating coils were weighed before and after the experiment. The depth of hard water scale was measured in millimeters and pictures of each pipe were taken for visual comparison. The boiler system with magnetic fluid treatment appeared to have about 2.5 times less scaling than the control according to weighing, measuring, and visually observing certain sections of the systems. A similar study involved using magnetic fluid treatment with a membrane distilling system. Gryta (2011) used commercial permanent magnetic systems with 0.1 Tesla each that were attached during the experimental runs. The scale observed with the magnet-treated sample was more porous with larger crystallites and in smaller amounts than the scale from the control. Physically measuring the amount of scale and visually observing the properties led most researchers to conclude that magnetic water treatment did reduce scaling. However, these experimental designs often failed to involve statistical analysis of multiple replications that could show that the amount of scaling reduction was statistically significant.

Calcium carbonate has three major phases: aragonite with needle-like crystals, calcite with rhombohedral crystals, and vaterite with spherical crystals. Vaterite is the least stable form while calcite is the most stable at ambient conditions. Aragonite formation favors higher temperatures. Aragonite and vaterite recrystallize to calcite over time. Calcite, because of its structure, is believed to form hard adhesive deposits that are the primary cause of hard water scaling. Some scientists believe that magnetic water treatment favors the formation of porous, soft, and soluble aragonite deposits, which reduces scaling issues (Lipus and Dobersek, 2007). Using X-ray diffraction, scanning electron microscopy, and microscopy analysis, Coey and Cass

(2000) identified the forms of the calcium carbonate deposits to see if magnetic fields promoted one structure over the other. The ratio of calcite to aragonite was evaluated by measuring the ratio of calcite at peak 104 and aragonite at peaks 111 and 102 using X-ray reflections in the region  $25^\circ < 2\theta < 30^\circ$ . Still mineral water and well water were treated separately. The samples were contained in polythene bottles and passed through either a bypass valve or a 0.1 Tesla permanent magnet system. More than 100 samples were blindly treated so the experimenter did not know which samples received the magnetic fluid treatment. Because of the experimental design, they were able to state with a 99.9% probability level that the magnetic fluid treatment increased the amount of aragonite in the deposits.

Fathi et al. (2006) analyzed magnetically treated water under a scanning electron microscope, and also observed that the magnetic field caused calcite and vaterite to form aragonite. Lipus and Dobersek (2007) showed in their hot water heater experiment reduced scaling with magnetic fluid treatment. The scaling in both hot water heaters was tested for aragonite using X-ray diffraction spectroscopy. The scientists concluded that aragonite did not reduce scaling because aragonite was the primary scaling component for both treatments.

Knez and Pohar (2005) passed water through an electromagnetic chamber and deduced that magnetic induction and exposure time had a notable influence on the amount of aragonite during magnetic fluid treatment but velocity was not an important factor. Coey and Cass (2000) reported a significant amount of aragonite with magnetic fluid treatment as well. Although not all studies directly link aragonite to scale prevention, some of the studies noticed an increased presence of aragonite with magnetic fluid treatment. The form of calcium carbonate being altered while exposed to a magnetic field can be proof that the water's properties have been influenced.



Changes in electric conductivity of water was used as an indicator that properties of the water molecules have been altered by magnetic fluid treatment. Pang and Deng (2008) conducted an experiment in which the electric conductivity of water samples was measured before and after being exposed to a static magnetic field. They exposed pure water, water with an insignificant amount of impurities, to a static magnetic field with a strength of 0.44 Tesla for 30min. The electric conductivity was measured for the control and magnetically treated sample with a semiconductor instrument. The electrical conductivity of the water was reported to be higher after treatment. The experimenters linked the increased electrical conductivity to an increase in charged particles created by the magnetic field.

Holysz et al. (2007) exposed model electrolyte solutions to a weak static permanent magnetic field, 0.015 Tesla, for five minutes. The electrolyte solutions were composed of inorganic salts including sodium chloride, potassium chloride, calcium chloride, and sodium phosphate dissolved separately in distilled water. After the treatment, the samples were allowed to rest for 30min prior to being measured for electrical conductivity with a multiparametric system. A change in electrical conductivity was observed in all of the electrolyte solutions. This change was linked to the nature of the ions changing. According to Holysz et al. (2007), the change in electrical conductivity was “proportional to the thickness of the hydration shell around the ions and thermodynamic functions of hydration.”

Surface tension has been used to measure physicochemical changes in water from magnetic fluid treatment but this method can be very susceptible to sources of error including solution contamination and instrumental limitations. Cai et al. (2009) pumped purified water at one meter per second through a permanent magnetic system with a magnetic flux density of one Tesla for 3 - 40h. The surface tensions of the control and treated samples were measured at room

temperature and a relative humidity of 40 - 50% by the plate method with a tensiometer, whose precision was 0.01mN/m. The magnetic field decreased the surface tension of the water from about 73mN/m to 66mN/m after thirteen minutes of magnetic exposure. Cai et al. (2009) suggested that the lower surface tension was the result of the molecular energy of the water decreasing from being exposed to the magnetic field.

Pang and Deng (2008) noticed a decrease in surface tension with magnetic fluid treatment as well using a micro optical-vision instrument. However, they attributed this observation to the magnetic field lowering the angles of contact for the water. Amiri and Dadkhah (2006) performed the most in-depth surface tension study of magnetically treated water. More than 200 tests were performed during which the surface tension over time after the treatment was taken into account. Deionized water was passed through a commercial magnetic system and the surface tension was recorded using a tensiometer. Amiri and Dadkhah (2006) found that the surface tension of water was too sensitive to experimental conditions to be considered as a reliable indicator of the effects of magnetic fluid treatment on water. A few studies have linked changes in surface tension to the magnetic fields altering the molecular structure of water. However, scientists who attribute changes to the surface tension to this cause do not agree on a mechanism that would explain the phenomenon. Therefore, surface tension may not be a reliable indicator for the effectiveness of magnetic fluid treatment.

Viscosity is another physicochemical property of water that has been measured to observe how water reacts in the presence of a magnetic field. Viscosity was measured when Cai et al. (2009) pumped water through a permanent magnet experiment using a rheometer. The magnetic fluid treatment increased the viscosity of the water. Cai et al. (2009) suggested that their observation was the result of the water's activation energy increasing from the treatment.

Pang and Deng (2008) used a micro optical-vision instrument to observe changes in viscosity for their static magnetic field water treatment experiment. An increase in viscosity with increasing magnetic fluid treatment was observed and assumed to be the result of additional hydrogen bonds being formed under the influence of the magnetic field. Viscosity measurement methods have both linked magnetic fluid treatments to alterations of the structure of water. However, viscosity measurements are not common for evaluating the effectiveness of magnetic fluid treatment.

### ***Proposed Magnetic Fluid Treatment Mechanisms***

Discovering the mechanism behind how a magnetic field influences the structure of water can be important to justify or explain any changes from magnetic fluid treatment. One theory assumes that the magnetic field changes the hydrogen bonds in the water and changes how water molecules become oriented around an ion within a hydration shell. Holysz et al. (2007) noticed that water exposed to the magnetic field experienced changes in its electric conductivity and evaporation rate. These changes depend on the type of ions present in the solution and are proportional to the hydration shell thickness around the ions and the thermodynamic functions of hydration. Therefore, Holysz et al. (2007) theorized that a magnetic field alters the hydration shell to cause a decrease in scaling. Changes in the hydrogen's bonding abilities during the magnetic fluid treatment were seen as the cause for an increase in the evaporation rates of the treated samples during the study as well.

Cai et al. (2009) observed nuclear magnetic resonance (NMR) relaxation measurements in water exposed to a magnetic field. The magnetic fluid treatment appeared to increase the activation energy of the water molecules, according to the NMR relaxation results. Cai et al. (2009) claimed that the change of molecular energy was an indicator of hydrogen bonds forming,

breaking, or reorienting. The more hydrogen bonds that form in water, the more inactive water is. The increase in hydrogen bonds caused the mean size of water clusters to increase as well from the magnetic fluid treatment (Cai et al., 2009). Changes in the ability of water molecules to interact with other water molecules and ions do help explain some of the observations made during magnetic water treatment studies. However, the mechanism by which the magnetic field changes these water properties has not been elucidated.

Kney and Parsons (2006) and Madsen (2004) suggested that the magnetic field alters the proton spin of water molecules instead of the hydration shell or hydrogen bonds. The magnetic field, according to this proposed mechanism, could influence the proton spin of water molecules which causes a faster proton transfer of bicarbonate ions to water. This results in a higher nucleation rate for crystals and reduced crystal size (Kney and Parsons, 2006). Madsen (2004) stated that proton spin relaxation occurs due to the theory of magnetic resonance spectroscopy. The proton spin relaxation mechanism is not supported by as much analytical analysis compared to the hydration shell and hydrogen bonding mechanisms because it stems from mostly observations of the resulting crystal size from magnetic fluid treatment. However, this mechanism is more direct in how the property changes in the water relate to the observed changes in the crystal formations.

Lorentz force acts upon any charged particles when they move through a magnetic field. The equation for the Lorentz force is  $F = qvB$  where  $F$  is the resulting force,  $q$  is the electrical charge of the particle,  $v$  is the velocity vector, and  $B$  is the magnetic field strength (Madsen, 2007). Theoretically, having the water flow orthogonal to the magnetic field will produce the highest force on the water molecules. Some scientists hypothesize that the Lorentz force is responsible for any observations related to changes in calcium carbonate compounds when water

is passed through a magnetic fluid treatment device (Kozic and Lipus, 2003). There are multiple theories for how the Lorentz force influences the water or dissolved ions. According to Fathi et al. (2006), this force could be capable of disturbing “the double ionic layer surrounding the colloidal particles and their zeta potential.” According to Alimi et al. (2009) “Lorentz forces exerted on charged species induce local convection movements in the liquid which could contribute to accelerate associations between ions or colloidal particles.”

Li et al. (2007) suggested that the resulting Lorentz force of the water moving through a magnetic field causes local ionic concentrations that modify the shape of calcium carbonate formations to promote more aragonite crystals. Madsen (2007) used the Lorentz force equation along with a mathematical model to show that theoretically any resulting Lorentz force should be too weak to have a notable influence on an aqueous system. Lorentz force might contribute to the scale reduction during magnetic fluid treatment but it does not explain why changes occur with static magnetic treatment.

A less popular theory proposes that the magnetic field enhances the corrosion of iron leading to free iron corrosion products (Busch and Busch, 1997). These products serve as nucleation centers for calcium carbonate. Thus, the hard precipitate will be suspended in the liquid instead of on surfaces (Coey and Cass, 2000). Botello-Zubiate et al. (2003) passed water through a one Tesla magnetic field at a rate of 0.77m/s and measured the corrosion behavior of the treated water using electrochemical polarization curves and steel corrosion as an example. The corrosion rates increased with magnetic water treatment. This theory, however, does not explain why magnetic water treatment studies with electrolyte solutions and purified water without iron or other metal ions still experienced changes. The mechanism for how the magnetic field speeds up the corrosion process also is not explained.

### ***Conclusions on Magnetic Fluid Treatment as a Feasible Physical Treatment***

Several scientific studies have reported changes in water properties from magnetic fluid treatment that could suggest that magnetic fields can reduce hard water scaling. Not all of the properties measured, especially aragonite content and surface tension, appear to be widely accepted as measures confirming the success of magnetic water treatment. Most of the experimental designs do not support statistical analysis because of too few replications, which might help to explain reports of poor reproducibility of results. The proposed mechanisms also are not supported by any in-depth analysis. The differences in experimental design for each study make it difficult to compare and draw conclusions from multiple studies. These differences include type of sample used, properties of the magnetic system, length of treatment, sample containers, and whether the sample was passed through the magnetic field.

More efforts focused on identifying the mechanism as well as experimental designs that would allow statistical analysis are needed. Researchers also need to collaborate to a greater degree to find the best experimental conditions and testing methods. Despite a lack of reliability with a fraction of the magnetic water treatment studies, magnetic fluid treatment has been reported to have potential in altering mineral composition and altering water properties, including surface tension and viscosity. Therefore, more studies involving magnetic fluid treatment are needed to find the appropriate treatment conditions and to explore any other applications of this physical treatment.

## **Conclusion**

Greek yogurt whey (GYW), because of its nutritional content, poses both an environmental issue and the potential for concentrating dairy components for other uses. Magnetic fluid treatment and the addition of sepiolite clay could be cost-effective methods to concentrate GYW components, especially minerals. Neither method has been extensively used with fluids chemically similar to GYW. There is not much research on sepiolite reacting with proteins, sugars, or minerals. The research regarding magnetic fluid treatment is very inconsistent with little agreement on the experimental parameters. The lack of reliable and relatable literature for both treatment methods makes predicting any results when applying them to GYW difficult. However, they still could be effective value-adding methods for GYW.

## Tables

**Table 1.1 Greek yogurt whey compositional analysis (U.S. Dairy Export Council, Arlington, VA, personal communication)**

	pH	Titrateable Acidity (%)	Total Protein (%)	Carbohydrates (%)	Lactose (%)	Lactic Acid (%)	Total Solids (%)	Ash (%)	Calcium (mg/100g)	Sodium (mg/100g)	Phosphorus (mg/100g)	Galactose (%)
Minimum	4.11	0.38	0.18	3.00	3.23	0.61	4.67	0.52	107.00	43.30	59.00	0.50
Average	4.45	0.42	0.27	4.41	3.53	0.70	5.77	0.72	120.12	50.47	66.37	0.61
Maximum	4.73	0.49	0.36	5.20	4.26	0.84	6.65	0.92	143.00	58.90	75.80	0.77



**Table 1.2 Summary of magnetic water treatment studies using permanent magnets**

Article	Substance Treated	Magnetic Field Strength	Flow Rate/ Velocity	Magnetic Exposure/ Run Time	Observations
(Coey and Cass, 2000)	Well Water and Mineral Water	0.1 Tesla	Static	1 pass	Magnetic treatment increases the amount of aragonite in water with a 99.9% level of probability. Effects last for over 200h.
(Botello-Zubiate et al., 2003)	Tap Water	1 Tesla	0.0936L/min	1 pass	Magnetic treatment favors the formation of aragonite and increases the corrosion rate of carbon steel.
(Chibowski et al., 2003)	Calcium Carbonate Solutions	0.1 Tesla	Static	2h	Magnetic treatment decreases calcium carbonate formation on surfaces including stainless steel, copper, aluminum, and glass despite the material or temperature.
(Holysz et al., 2003)	Calcium Carbonate Solutions	0.5 Tesla	Static	20min	Magnetic treatment influenced the zeta potential of calcium carbonate as well as the light absorbance and pH of the treated solutions. The presence of impurity ions including magnesium, iron, and sulfate influenced the effects of magnetic treatment.
(Kney and Parsons, 2006)	Electrolyte Solutions	0.55 Tesla	Static	16 to 30min	Magnetic treatment had an effect on solutions made with calcium carbonate but not with solutions made with sodium carbonate.
(Amiri and Dadkhah, 2006)	Tap and Purified Water	0.385 Tesla	Gravity	1 pass	Surface tension is not a reliable indicator for determining the influence of a magnetic field on water properties.
(Fathi et al., 2006)	Calcium Carbonate Solutions	0.16 Tesla	Laminar region	5 to 30min	Magnetic treatment increases homogeneous nucleation of calcium carbonate. The effect is promoted by an increase in pH, increase in flow rate, and an increase in the residence time.
(Alimi et al., 2007)	Calcium Carbonate Solutions	0.16 Tesla	0.50, 0.74, and 0.94L/min	15min	Magnetic treatment caused more nucleation of calcium carbonate in the bulk solution. Higher flow rates and higher pH values increased this effect.
(Holysz et al., 2007)	Electrolyte Solutions	0.015 Tesla	Static	0 to 80min	Magnetic treatment influenced the conductivity and amount of water evaporated in the solutions.
(Lipus and Dobersek, 2007)	Tap Water	0.6 - 0.8 Tesla	0.2L/min	0.1s	Magnetic treatment reduces hard water scale formation in hot water boilers. The formation of aragonite was not the cause for the decrease in hard scale formation.
(Xiao-Feng and Bo, 2008)	Purified Water	0.44 Tesla	Static	0 to 75min	Magnetic treatment increases the soaking degree, depresses surface tension, increases the electric conductivity, and increases the refraction index of water.
(Alimi et al., 2009)	Calcium Carbonate Solutions	0.16 Tesla	0.54, 0.74, and 0.94L/min	15min	Magnetic treatment decreases hard scale formation despite the pipe material including PTFE, TYGON, PVC, copper, and stainless steel.
(Cai et al., 2009)	Purified Water	0.50 Tesla	1m/s	3 to 40h	Magnetic treatment decreases the surface tension and increases the viscosity over treatment time.
(Gryta, 2011)	Calcium Carbonate Solutions	0.1 Tesla	0.07m/s	45 passes	Magnetic treatment reduced the amount of hard water scale formation on membranes for membrane filtration. The main formation of calcium carbonate was calcite.

**Table 1.3 Summary of magnetic water treatment studies using electric magnets**

Article	Substance Treated	Magnetic Field Strength	Flow Rate/ Velocity	Magnetic Exposure/Run Time	Observations
(Strazisar et al., 2001)	Calcium Carbonate Solutions	0.5 - 1.3 Tesla	0L/min and 0.03L/min	1 to 10h	Magnetic treatment does not influence the zeta potential of calcium carbonate. The magnetic field favors the formation of aragonite. Static and dynamic treatment gave similar results.
(Kobe et al., 2003)	Calcium Carbonate Solutions	0.0004 - 0.0015 Tesla	0.87m/s	8h	Magnetic treatment influences the formation of calcium carbonate crystals. The magnetic field strength, flow rate, and presence of impurity ions including copper and silicon are important parameters for treatment.
(Cho and Lee, 2004)	Hard Water	0.16 Tesla	1.0m/s and 6.3m/s	30 passes	Magnetic treatment decreases the surface tension of water despite the type of magnet that produced the magnetic field.
(Knez and Pohar, 2005)	Calcium Carbonate Solutions	0.71 - 1.12 Tesla	0.1 to 3L/min	4.2 to 8.4min	Magnetic treatment favored the formation of aragonite but did not alter the zeta potential of calcium carbonate. Treatment was dependent on magnetic induction and magnetic exposure time but fluid velocity was not a significant parameter.
(Madsen, 2004)	Calcium Carbonate Solutions	0.25 Tesla	None	30min	Magnetic treatment decreases calcium carbonate crystal size. High pH values hinder the treatment effects.
(Li et al., 2007)	Calcium Carbonate Solutions	0.02 Tesla	Low	2h	Magnetic treatment favors the formation of calcite to vaterite or aragonite. The treatment causes less fouling in membrane filtration systems.

## References

- Alimi, F., M. Tlili, M. Ben Amor, C. Gabrielli, and G. Maurin. 2007. Influence of magnetic field on calcium carbonate precipitation. *Desalination*. 206:163–168.
- Alimi, F., M.M. Tlili, M.B. Amor, G. Maurin, and C. Gabrielli. 2009. Effect of magnetic water treatment on calcium carbonate precipitation: influence of the pipe material. *Chem. Eng. Process*. 48:1327–1332.
- Alsaed, A.K., R. Ahmad, H. Aldoomy, S. Abd El-Qad, D. Saleh, H. Sakejha, and L. Mustafa. 2013. Characterization, concentration and utilization of sweet and acid whey. *Pakistan J. Nutr*. 12:172–177.
- Ambashta, R.D., and M. Sillanpää. 2010. Water purification using magnetic assistance: a review. *J. Hazard. Mater*. 180:38–49.
- Amiri, M.C., and A.A. Dadkhah. 2006. On reduction in the surface tension of water due to magnetic treatment. *Colloids Surf. A Physicochem. Eng. Asp*. 278:252–255.
- Botello-Zubiate, M.E., A. Alvarez, A. Martínez-Villafañe, F. Almeraya-Calderon, and J.A. Matutes-Aquino. 2004. Influence of magnetic water treatment on the calcium carbonate phase formation and the electrochemical corrosion behavior of carbon steel. *J. Alloys Compd*. 369:256–259.
- Brigatti, M.F., P. Frigieri, C. Gardinali, L. Medici, L. Poppi, and G. Franchini. 1999. Treatment of industrial wastewater using zeolite and sepiolite, natural microporous materials. *Can. J. Chem. Eng*. 77:163–168.
- Busch, K.W., and M.A. Busch. 1997. Laborator studies on magnetic water treatment and their relationship to a possible mechanism for scale reduction. *Desalination*. 109:131–148.
- Bylund, G. 2003. *Dairy Processing Handbook*. Tetra Pak Processing Systems AB. 27–34, 415–423 pp.
- Cai, R., H. Yang, J. He, and W. Zhu. 2009. The effects of magnetic fields on water molecular hydrogen bonds. *J. Mol. Struct*. 938:15–19.
- Chandan, R.C., A. Kilara, and N. Shah. 2008. *Dairy Processing and Quality Assurance*. 1 ed. Wiley-Blackwell, Ames, Iowa. 41–58 pp.
- Chandan, R.C., and A. Kilara. 2010. *Dairy Ingredients for Food Processing*. Blackwell Publishing Ltd., Ames, Iowa. 64–68 pp.
- Chibowski, E., L. Hołysz, and A. Szcześ. 2003. Adhesion of in situ precipitated calcium carbonate in the presence and absence of magnetic field in quiescent conditions on different solid surfaces. *Water Res*. 37:4685–4692.

- Cho, Y.I., and S.-H. Lee. 2005. Reduction in the surface tension of water due to physical water treatment for fouling control in heat exchangers. *Int. J. Heat Mass Transf.* 32:1–9.
- Coey, J.M.D., and S. Cass. 2000. Magnetic water treatment. *J. Magn. Magn. Mater.* 209:71–74.
- Corredig, M. 2009. *Dairy-Derived Ingredients: Food and Nutraceutical Uses*. 1 ed. Woodhead Publishing, Boca Raton; Cambridge. 110–112 pp.
- Demirel, B., O. Yenigun, and T.T. Onay. 2005. Anaerobic treatment of dairy wastewaters: a review. *Process Biochem.* 40:2583–2595.
- Desai, N.T., L. Shepard, and M.A. Drake. 2013. Sensory properties and drivers of liking for Greek yogurts. *J. Dairy Sci.* 96:7454–7466.
- Doğan, M., Y. Özdemir, and M. Alkan. 2007. Adsorption kinetics and mechanism of cationic methyl violet and methylene blue dyes onto sepiolite. *Dyes and Pigm.* 75:701–713.
- Erdem, A., F. Kuralay, H.E. Çubukçu, G. Congur, H. Karadeniz, and E. Canavar. 2012. Sensitive sepiolite-carbon nanotubes based disposable electrodes for direct detection of DNA and anticancer drug–DNA interactions. *Analyst.* 137:4001–4004.
- Esteban-Cubillo, A., J.-M. Tulliani, C. Pecharromás, and J.S. Moya. 2007. Iron-oxide nanoparticles supported on sepiolite as a novel humidity sensor. *Eur. Ceram. Soc.* 27:1983–1989.
- Fathi, A., T. Mohamed, G. Claude, G. Maurin, and B.A. Mohamed. 2006. Effect of a magnetic water treatment on homogeneous and heterogeneous precipitation of calcium carbonate. *Water Res.* 40:1941–1950.
- Goff, J.P. 2006. Major advances in our understanding of nutritional influences on bovine health. *J. Dairy Sci.* 89:1292–1301.
- Gryta, M. 2011. The influence of magnetic water treatment on CaCO<sub>3</sub> scale formation in membrane distillation process. *Sep. Purif. Technol.* 80:293–299.
- Guney, Y., B. Cetin, A.H. Aydilek, B.F. Tanyu, and S. Kopal. 2014. Utilization of sepiolite materials as a bottom liner material in solid waste landfills. *Waste Manag.* 34:112–124.
- Haug, A., A.T. Høstmark, and O.M. Harstad. 2007. Bovine milk in human nutrition: a review. *Lipids Health Dis.* 6:25–41.
- Hołysz, L., E. Chibowski, and A. Szcześ. 2003. Influence of impurity ions and magnetic field on the properties of freshly precipitated calcium carbonate. *Water Res.* 37:3351–3360.
- Hołysz, L., A. Szczech, and E. Chibowski. 2007. Effects of a static magnetic field on water and electrolyte solutions. *J. Colloid Interface Sci.* 316:996–1002.

- Kang, E.J., T.J. Smith, and M.A. Drake. 2012. Alternative bleaching methods for cheddar cheese whey. *J. Food Sci.* 77:C818–C823.
- Keller, A.K., inventor. 2015. Process and system for drying acid whey. Proliant Dairy Inc., assignee. US Pat. App. No. 13/974,718.
- Kney, A.D., and S.A. Parsons. 2006. A spectrophotometer-based study of magnetic water treatment: assessment of ionic vs. surface mechanisms. *Water Res.* 40:517–524.
- Knez, S., and C. Pohar. 2005. The magnetic field influence on the polymorph composition of CaCO<sub>3</sub> precipitated from carbonized aqueous solutions. *J. Colloid Interface Sci.* 281:377–388.
- Kobe, S., G. Dražić, A.C. Cefalas, E. Sarantopoulou, and J. Stražišar. 2002. Nucleation and crystallization of CaCO<sub>3</sub> in applied magnetic fields. *Cryst. Eng.* 5:243–253.
- Kosseva, M., and C. Webb. 2013. *Food Industry Wastes*, 1st Ed. Academic Press, Elsevier, San Diego, USA. 37–56 pp.
- Kozic, V., J. Kropc, L.C. Lipus, and I. Ticar. 2006. Magnetic field analysis on electromagnetic water treatment device. *Hungarian J. Ind. and Chem.* 34:51–54.
- Kozic, V., and L.C. Lipus. 2003. Magnetic water treatment for a less tenacious scale. *J. Chem. Inf. Comput. Sci.* 43:1815–1819.
- Li, J., J. Liu, T. Yang, and C. Xiao. 2007. Quantitative study of the effect of electromagnetic field on scale deposition on nanofiltration membranes via UTDR. *Water Res.* 41:4595–4610.
- Lipus, L.C., and D. Dobersek. 2007. Influence of magnetic field on the aragonite precipitation. *Chem. Eng. Sci.* 62:2089–2095.
- Madsen, H.E.L. 2007. Theory of electrolyte crystallization in magnetic field. *J. Cryst. Growth.* 305:271–277.
- Mousty, C. 2004. Sensors and biosensors based on clay-modified electrodes: new trends. *Appl. Clay Sci.* 27:159–177.
- Nsabimana, C., B. Jiang, and R. Kossah. 2005. Manufacturing, properties and shelf life of labneh: a review. *Int. J. Dairy Technol.* 58:129–137.
- Özcan, A., E.M. Öncü, and A.S. Özcan. 2006. Kinetics, isotherm and thermodynamic studies of adsorption of Acid Blue 193 from aqueous solutions onto natural sepiolite. *Colloids Surf. A Physicochem. Eng. Asp.* 277:90–97.
- Pang, X.-F., and B. Deng. 2008. The changes of macroscopic features and microscopic structures of water under influence of magnetic field. *Physica B Condens. Matter.* 403:3571–3577.

- Parisini, P., G. Martelli, L. Sardi, and F. Escribano. 1999. Protein and energy retention in pigs fed diets containing sepiolite. *Anim. Feed Sci. Technol.* 79:155–162.
- Pettigrew, J.E., and M.A. Esnaola. 2001. Swine nutrition and pork quality: A review. *J. Anim. Sci.* 79:E316–E342.
- Power, M.L., R.P. Heaney, H.J. Kalkwarf, R.M. Pitkin, J.T. Repke, R.C. Tsang, and J. Schulkin. 1999. The role of calcium in health and disease. *Am. J. Obstet. Gynecol.* 181:1560–1569.
- Sarkar, B., P.P. Chakrabarti, A. Vijaykumar, and V. Kale. 2006. Wastewater treatment in dairy industries: possibility of reuse. *Desalination.* 195:141–152.
- Schultx, E.J., and R. Parekh. 2011. Strong consumer demand pushes Greek yogurt into a dairy-aisle battlefield. Accessed Nov. 1, 2014. <http://adage.com/article/news/greek-yogurt-sparks-a-dairy-aisle-battlefield/149351>.
- Strazisar, J., S. Knez, and S. Kobe. 2001. The influence of the magnetic field on the zeta potential of precipitated calcium carbonate. *Part. Part. Syst. Charact.* 18:278–285.
- Tekbaş, M., N. Bektaş, and H.C. Yatmaz. 2009. Adsorption studies of aqueous basic dye solutions using sepiolite. *Desalination.* 249:205–211.
- Wail-Alomari, A.K. Alsaed, and M. Hadadin. 2012. Utilization of *labneh* whey lactose hydrolyzed syrup in baking and confectionery. *Pakistan J. Nutr.* 11:786–793.

## **Chapter 2 - Research Objectives**

1. To briefly explain how Greek yogurt whey properties lead to the need to develop alternative treatment methods
2. To determine the chemical and physical composition of Greek yogurt whey from two commercial sources
3. To evaluate two physical treatments, magnetic fluid treatment and the addition of sepiolite, as methods for adding value to Greek yogurt whey

## **Chapter 3 - Magnetic Fluid Treatment and Sepiolite Addition as Methods for Concentrating Greek Yogurt Whey Components**

### **Abstract**

The demand for Greek yogurt in the United States is steadily increasing. Consequently, the co-product of Greek yogurt processing, Greek yogurt whey, has an acidic pH, high mineral content, and low protein content that make traditional whey processing methods difficult and uneconomical. Magnetic fluid treatment and the addition of a magnesium hydrosilicate clay mineral, sepiolite, were evaluated as physical cost-effective methods to add value to Greek yogurt whey. Three separate batches of Greek yogurt whey were obtained from two United States Greek yogurt manufacturers. A Greek yogurt whey sample was collected from each batch, adjusted to a pH of 7.2, and re-circulated for five minutes through a pumping system at a rate of 7.5L/min with or without exposure to a permanent magnetic field. The magnetic field had a peak field strength of 0.6T. The sample was split into thirds, heated to 80°C, and then sepiolite was added at one of three levels: zero, two, or four grams of sepiolite per 100g Greek yogurt whey. After centrifugation at 1,000g for five minutes, the samples formed a top aqueous and a bottom sediment layer. The top aqueous layers were analyzed for total solids (TS), ash, lactose, protein, calcium, phosphates, and sodium contents along with color. Magnetic fluid treatment did not affect the analyzed Greek yogurt whey components from both manufacturers ( $P > 0.05$ ) except for the lactose content of the top aqueous layers from manufacturer 2. The addition of sepiolite had the greatest effect on the phosphate and protein content along with color for the top aqueous layers. The addition of sepiolite significantly lowered the phosphate concentration in the top aqueous layers for both manufacturers ( $P < 0.05$ ). Protein within the top aqueous layers compared to Greek yogurt whey significantly decreased about 60% for manufacturer 1 and 45%



for manufacturer 2 with either amount of sepiolite treatment ( $P < 0.05$ ). The color values  $b^*$  and  $a^*$  in the Greek yogurt whey from both manufacturers significantly decreased with the addition of sepiolite by about 70% and 90%, respectively ( $P < 0.05$ ). The adsorption of protein was contributed to electrostatic effects while the adsorption of the color pigments was contributed to sepiolite's large surface area. Magnetic fluid treatment and sepiolite addition under the conditions in the present study were not practical treatment methods for de-mineralizing Greek yogurt whey. However, sepiolite was found to have possible applications in the removal of proteins and natural color pigments in Greek yogurt whey.

## Introduction

Greek yogurt accounts for over 25% of American yogurt sales and its demand has continued to rise. Greek yogurt or strained yogurt is obtained by removing a portion of the water and water soluble components, Greek yogurt whey (GYW), from yogurt (Desai et al., 2013). The co-product GYW accounts for about two-thirds of the original milk that goes into the manufacture of Greek yogurt. GYW has the following average composition 4.45 pH, 5.77% total solids (TS), 0.72% ash, 3.53% lactose, and 0.27% total protein (U.S. Dairy Export Council, Arlington, VA, personal communication). Acid whey from cottage cheese typically has the following characteristics 6.4% TS, 0.75% ash, 4.6% lactose, 0.7% total protein, and pH of 4.5 (Chandan and Kilara, 2010). GYW on average can be more acidic than acid whey from cottage cheese manufacturing and contains notably less protein and lactose. Even though GYW has an acidic pH, it cannot be correctly classified as acid whey because it is compositionally different.

The characteristic low pH and high mineral content of GYW creates issues with equipment fouling. GYW is difficult to dry into a free-flowing powder using traditional drying methods because it contains a relatively high amount of hygroscopic components including lactic acid and galactose formed during Greek yogurt manufacturing. GYW contains small amounts of high-molecular-weight proteins and lactose monohydrate that typically aid in the drying process (Keller, 2015). Besides drying concerns, GYW, unlike acid whey, is lower in value due to its lower protein and lactose contents. Even without the processing concerns, it is not economically feasible to treat GYW with traditional methods. Disposal methods for GYW include land application, bioreactors, and animal feed but each of these methods has its own limitations and adds little value to the GYW (U.S. Dairy Export Council, Arlington, VA, personal communication). In March 2015, the U.S. Dairy Export Council released a report that included

its goal to investigate potential opportunities for GYW. Finding low-cost methods of adding value to GYW or fractionating the valuable components is needed.

Clay minerals are natural low-cost adsorbents of dye, proteins, and heavy metals.

Sepiolite is a natural clay mineral with the following unit-cell formula

$(\text{Si}_{12})(\text{Mg}_8)\text{O}_{30}(\text{OH})_4(\text{OH}_2)_4 \cdot 8\text{H}_2\text{O}$ . It is classified as a magnesium hydrosilicate and is composed of blocks consisting of two tetrahedral silica sheets enclosing a central octahedral magnesia sheet. The mineral's structure is responsible for its high specific surface area, molecular-sized channels, high stability, and its ability to adsorb both organic and inorganic ions. Sepiolite reserves are abundant in Turkey and can also be found in parts of the United States including Nevada and California. Sepiolite is commonly used in the production of paint, paper, cosmetics, and detergents (Doğan et al., 2007). Guney et al. (2013) discovered that sepiolite has applications as a liner for landfills because of its effectiveness at adsorbing heavy metals including lead, copper, and zinc. Sepiolite has also proven effective at removing various dyes from color effluents: Basic Astrazon yellow 7GL, methylene blue, and methyl violet (Tekbaş et al., 2009). The structural properties and abundant supply of sepiolite has made it a cost-effective solution for treating various forms of industrial waste-streams.

Magnetic fluid treatment (MFT) is a possible cost-effective physical treatment for separating mineral components. MFT was initially researched as a method to reduce hard water scaling caused by calcium carbonate deposits. Reported claims for exposing water to a magnetic field include lower scale formation rate, development of soft scale formations, change in size of precipitated particles, and no significant effects (Strazisar et al., 2001). Controversy over the effectiveness of this treatment centers on both laboratory and industrial studies having low reproducibility, the existence of reports with conflicting results, and the lack of an accepted and

proven mechanism (Cai et al., 2009). Researchers suggest that magnet type, magnetic field strength and orientation, magnetic exposure time, flow rate of the sample, and pipe or container material could all be important factors for proper treatment (Holysz et al., 2007). MFT has the potential to alter characteristics of minerals but the lack of an agreed upon experimental setup or mechanism makes predicting any results difficult.

The objective of the present study was to examine sepiolite addition and MFT as cost-effective physical treatment methods for separating out or isolating valuable components in GYW including protein, lactose, and minerals. Separating these GYW components would aid in the disposal of this co-product while adding value. A treatment process was developed to observe if the addition of sepiolite would aid in the removal of minerals or other components made insoluble by MFT. These two methods were evaluated separately as alternative processing techniques for value addition of GYW as well.

## **Materials and Methods**

### ***Experimental Design***

Two commercial United States manufacturers of Greek yogurt supplied three separate Greek yogurt whey (GYW) batches collected from different processing days. Treatment included a 2×3 factorial design of two magnetic treatment levels, magnetic fluid treatment (MFT) and no exposure to the magnetic field, and three sepiolite treatment levels: the addition of zero, two, or four grams of sepiolite per 100g of sample. Each batch received duplicates of each of the eight clay and magnetic treatment combinations.

### ***MFT System Development***

The MFT chamber design shown in Figure 3.1 was based on operating conditions for proper magnetic water treatment suggested by Strazisar et al. (2001): the fluid flow is orthogonal with respect to magnetic field direction, magnetic field strength is at least 0.5 – 1 Tesla, there is a long residence time, and the water flow is turbulent.

Finite Element Method Magnetics (FEMM) 4.2 software (David Meeker, Charlottesville, VA) was used to determine the orientation of the magnets that would produce the strongest magnetic flux perpendicular to the fluid flow. The chosen design features four pairs of 5.08 x 2.54 x 5.08cm neodymium block permanent magnets (Stanford Magnets, Irvine, CA) placed with opposing poles across from each other. Parallel magnets were spaced 2.5cm from each other and had the opposite field orientation from the adjacent pairs. The magnetic field inside the magnetic chamber was measured with a gauss meter (DC Magnetometer (Gauss), AlphaLab Inc., Salt Lake City, UT).

The MFT system displayed in Figure 3.1 was designed to recirculate the sample through the magnetic field. The sample was loaded into a polypropylene funnel. The funnel fed the

sample into a centrifugal pump (Iwaki Magnet Pump Model # MD-15R-115NL01, Iwaki America Inc., Holliston, MA) which pushed the sample at a rate of 7.5L/min through a 1.27cm inner diameter stainless steel pipe. The magnetic chamber was attached to the stainless steel pipe. Teflon tubing with 1.27cm inner diameter carried the sample back to the funnel.

### ***Sepiolite***

Sepiolite, Sepiogel F, was obtained from IMV Nevada (Amargosa Valley, NV) as per manufacturer with 12.2% free moisture and a particle distribution of 4.6% > 325 mesh and 95.4% < 325 mesh. Particle chord length distribution of the sepiolite particles was confirmed using Focused Beam Reflectance Measurement (FBRM) (Particle Track E25, Mettler-Toledo LLC., Columbus, OH) as per the instrument manufacturer's instructions.

### ***Process Description: MFT and Sepiolite Addition***

For each run 1,500g of GYW sample was heated to 40 - 42°C using a hot plate with constant stirring. The pH of the samples was recorded at 40 - 42°C using a pH meter with a temperature probe (Accumet™ AP110 Portable pH Meter, Thermo Fisher Scientific, Waltham, MA). The pH of the sample was then adjusted to 7.20 - 7.25 using a 5N sodium hydroxide solution. About 11.50 – 22.70g and 10.00 - 10.25g of 5N sodium hydroxide solution was used to neutralize the GYW from manufacturer 1 and manufacturer 2, respectively.

The pH adjusted sample was processed through the MFT system for five minutes. The magnetic chamber was removed for control samples. The sample was collected from the pumping system, pH at 40 - 42°C recorded, and split into three 450g sub-samples. Each sub-sample was heated to 80 - 82°C with constant stirring and covered to avoid evaporation of the sub-sample. Once the sub-sample reached 80 - 82°C, the appropriate amount of sepiolite was added according to the experimental design and mixed for two minutes at 80 - 82°C.

Subsequently, the heated 450g sub-samples were placed immediately into 500ml polypropylene centrifuge bottles and centrifuged at 1,000g for five minutes with a centrifuge (J2-21, Beckman Coulter Inc., Brea, CA). Centrifugation resulted in two distinct layers being formed including a top aqueous layer and a bottom sediment layer. Both layers were weighed and stored separately at  $< -10^{\circ}\text{C}$  until further analysis. Figure 3.2 contains a flow diagram of the treatment process.

### ***Chemical and Physical Analysis***

Both layers were tested for TS, ash, calcium, phosphates, sodium, and protein contents. The top aqueous layers were tested for color and lactose content. Untreated GYW samples from each batch were tested for the components previously mentioned except for lactose content. Duplicate analysis was performed for each sample.

***Calcium.*** Calcium in the samples was analyzed with flame atomic absorption using the method described by Zucchetti and Contarini (1993) with some modifications. Sample, 0.7 - 0.8g, was mixed with 29.25ml of 12% trichloroacetic acid (TCA) and incubated at  $23^{\circ}\text{C}$  for 30min. The sample was filtered through filter paper (Whatman #541, GE Healthcare Bio-Sciences, Pittsburg, PA). Ten milliliters of filtrate was added to 0.40ml of 5% lanthanum oxide solution and appropriately diluted with double deionized water. The diluted sample was analyzed at 589nm with an atomic absorption spectrometer (AAAnalyst 100, PerkinElmer Inc., Waltham, MA).

***Sodium.*** Sodium analysis followed the sample procedure mentioned above for calcium analysis except the samples were analyzed at 589nm using atomic emission mode with an atomic absorption spectrometer (AAAnalyst 100, PerkinElmer Inc., Waltham, MA). The standard curve

for the sediment layers contained 0.1, 0.5, and 5.0ppm sodium standard solutions while 5.0, 10.0, and 25.0ppm sodium standard solutions were used for the top aqueous layers' standard curve.

**Color.** A colorimeter (HunterLab Mini Scan EZ Colorimeter Model # 4500L, Hunter Associates Laboratory Inc., Reston, VA) was used to obtain L\*, a\*, and b\* values for the GYW and treated top aqueous layers. Three readings were recorded for each sample.

**Lactose.** Lactose in the sample was measured using the method described by Amamcharla and Metzger (2011). One gram of sample was diluted with 20g of distilled water. Five milliliters of diluted sample were added to 0.1ml of lactase (Enzeco<sup>®</sup> Lactase NL, Enzyme Development Corp., New York, NY), mixed, and incubated at 40°C for ten minutes. The samples were mixed and measured using a blood glucose meter (ReliOn Ultima, Abbott Laboratories, Abbott Park, Illinois).

**Phosphate.** Phosphate content was determined using the colorimetric method from Fiske and Subbarow (1925). The absorbance of each sample was read at 660nm using a spectrometer (Spectronic Genesys 5, Thermo Fisher Scientific, Waltham, MA). Top aqueous layers of duplicate samples with the following ratios of two grams of sepiolite per 100g distilled water and four grams of sepiolite per 100g distilled water were prepared. The sepiolite and distilled water samples were then centrifuged at 1,000g for five minutes and used to determine the background color development for sepiolite-containing samples. Additional dilution was required for most samples.

**Total Nitrogen.** Total nitrogen was analyzed by combustion assay (Trumac N, LECO Corp., St. Joseph, MI). A conversion factor of 6.38 was used to determine the crude protein content from the total nitrogen.



**Total Solids and Ash.** TS for both layers was determined using the forced air method described by Wehr et al. (2004). Ash for both layers was determined using the incineration method described by Wehr et al. (2004).

### ***Identification of Proteins on the Sepiolite Surface***

Clay mineral surfaces are capable of adsorbing proteins; therefore florescent microscopy was used to determine if GYW proteins had an attraction to sepiolite surfaces. The whey proteins were stained by adding 5 $\mu$ L of sample to 2 $\mu$ L of Fast Green FCF. The samples were then observed using a laser scanning confocal microscope (LSM 5 Pascal, Carl Zeiss AG, Oberkochen, Germany) with a 560 – 615nm band-pass filter and a laser line of 543nm (Auty et al., 2001).

### ***Scanning Electron Microscopy (SEM)***

A scanning electron microscope (Nova NanoSEM 430, FEI Company, Hillsboro, OR) was used to observe the surface morphology of the GYW bottom sediment layers and the original sepiolite. The sepiolite with GYW samples were then observed under SEM with 10kV accelerating voltage. Sepiolite direct from the manufacturer was observed using both 5kV and 10kV accelerating voltage. Neither the sepiolite with GYW nor original sepiolite samples were dried prior to SEM imaging. The SEM contained an X-ray detector (X-Max Large Area Analytical EDS silicon drift detector, Oxford Instruments, Abingdon, Oxfordshire) for analysis of the elemental composition of the samples. X-ray elemental analysis was performed once per each sample type with a spot of 4.0 and an accelerating voltage of 15kV, and X-ray elemental analysis involved four interactions of the chosen area in order to achieve about 250,000 total counts.

### *Statistical Analysis*

A t-test was conducted comparing average composition values of the original GYW from both manufacturers collected from all the batches. The test was conducted using the proc ttest function with SAS software version 9.3 (SAS Institute Inc., Cary, NC) with significance tested at  $P < 0.05$ .

The statistical model was a Randomized Complete Block Design plus split plot with three blocks where each block was a batch of GYW. MFT was designated as the whole plot while sepiolite addition was the split plot. Analysis of Variance (ANOVA) for split plot was used to test compositional differences between each layer resulting from the treatments. Data were analyzed separately for each manufacturer using PROC MIXED with SAS software version 9.3 (SAS Institute Inc., Cary, NC) with significance tested at  $P < 0.05$ . Least Squared Means were used to compare effects of the levels of sepiolite addition.

## **Results and Discussion**

### ***Modeling of MFT Chamber***

In the MFT chamber as seen in Figure 3.1, the flow of GYW is always perpendicular to the magnetic field direction. However, the magnetic field direction changes 180° based on the orientation of the magnets. As the GYW flows through the MFT chamber, it experiences a magnetic field when it passes through a gap in-between a pair of magnets. According to Figure 3.3, the theoretical magnetic flux density sharply increases to a maximum of about 0.9 - 0.95 Tesla in the gap between the magnet pair. The actual magnetic flux density measured with a gauss meter was 0.6 Tesla. The difference between the theoretical and actual magnetic flux density could be the result of interference with the pipe materials between the magnets and the fluid and impurities within the magnets (Baltzis, 2009).

### ***Greek Yogurt Whey***

Table 3.1 shows the average chemical composition of the GYW used in the present study. Only the pH, L\*, and b\* values were significantly different between the GYW from both manufacturers ( $P < 0.01$ ). GYW from both manufacturers had the following general composition 6.03% TS, 0.73% ash, and 0.26% protein. The pH, TS, ash, protein, and calcium values fall into the range observed from a study that analyzed GYW from ten United States Greek yogurt manufacturing sites (U.S. Dairy Export Council, Arlington, VA, personal communication).

### ***Effect of Magnetic Field on GYW Components***

Results from the top aqueous layers were used to evaluate the effectiveness of the treatments. The high sepiolite content of the bottom sediment layers resulted in various issues including difficulty in obtaining a uniform sample of the bottom sediment layer. Also, the high amount of silica in the sepiolite rich bottom sediment layer caused interference with calcium

analysis (Zucchetti and Contarini 1993). Therefore, the discussion in the present study will focus on results from the top aqueous layers.

The composition of the top aqueous layers without any influence from the MFT was compared to the GYW from the manufacturers. Neutralizing and heating the GYW favored the formation of insoluble tricalcium phosphate from soluble monocalcium phosphate (Corredig 2009). Tricalcium phosphate and other insoluble GYW components were separated from the top aqueous layer during centrifugation. Removing the insoluble components lowered the calcium content in the GYW from both manufacturers by about 75%. Phosphate concentration (mM) was lowered about 70% for GYW from manufacturer 1 and about 55% for GYW from manufacturer 2. Percent protein was lowered about 40% for GYW from manufacturer 1 and about 25% for GYW from manufacturer 2. The added sodium from the sodium hydroxide solution could be a part of either the top aqueous layer or the bottom sediment layer which makes it difficult to compare the ash and sodium of the raw GYW to the GYW top aqueous layers with pH and temperature treatment. There were relatively high variations in pH between the GYW batches collected from manufacturer 1 compared to those collected from manufacturer 2. The GYW from manufacturer 1 required about twice the amount of 5N sodium hydroxide sodium for neutralization compared to the GYW from manufacturer 2. The high standard deviation for the sodium values from manufacturer 1 as seen in Table 3.2 are the result of the pH variation between the GYW batches and the additional amount of base solution required for neutralization. The chosen pH and temperature parameters were desirable for de-mineralizing the GYW.

There was no interaction between the MFT and the addition of sepiolite ( $P > 0.05$ ) for both manufacturers. Therefore, both treatments were observed separately for any differences in composition of the top aqueous layers. The MFT was not an effective method of precipitating

additional GYW minerals. MFT did not have an impact ( $P > 0.05$ ) on any of the analyzed properties of the GYW top aqueous layers from manufacturer 1 as seen in Table 3.2. GYW top aqueous layers from manufacturer 2 had a difference in the amount of lactose from MFT ( $P < 0.01$ ) as seen in Table 3.2. There were no other significant differences ( $P > 0.05$ ) from MFT with GYW from manufacturer 2. The compositional changes in the top aqueous layers exposed to MFT were a result of the temperature and pH conditions instead of influence from the magnetic field. The observation with lactose from manufacturer 2 might require further support because of the lack of differences experienced with all of the properties of both manufacturers from MFT.

The MFT not influencing the precipitated GYW minerals could be the result of the necessary experimental conditions not being met. It is unknown currently what parameters might aid in the precipitation of minerals in a fluid compositionally similar to GYW. Any combination of the GYW composition, magnet type, magnetic field strength, or exposure time along with unknown factors could be the cause. Lipus and Dobersek (2007) used MFT on hard water in a hot water heater and observed a structural change in calcium carbonate from calcite to aragonite as a result of the MFT treatment. However, MFT did not change the amount of scaling in the hot water heater. Therefore, MFT might alter the structure of minerals but not their solubility. The ideal conditions for MFT of GYW need to be examined further if this method is to be a proposed solution for removing GYW minerals.

### ***Effect of Sepiolite Addition***

FBRM was used to observe the chord length distribution of the sepiolite particles. The chord length was found to be around  $20\mu\text{m}$ . The average particle size was  $44\mu\text{m}$  according to manufacturer specifications. Özcan et al. (2006) reported a surface area of  $234.3\text{m}^2/\text{g}$  for sepiolite passed through a  $63\mu\text{m}$  sieve. Smaller sepiolite particles have a larger surface area and

thus a great capacity to adsorb organic and inorganic materials. Observed sepiolite particles in the present study had large surface areas and identifiable channels as seen in Figure 3.4. This is consistent with the nature of this material. The particle size distribution is dependent on any size reduction processing but the morphology of the mineral remains unchanged. How the properties of sepiolite attract GYW components was evaluated in the present study.

The lactose content of the top aqueous layers was independent of sepiolite addition for manufacturer 1 ( $P = 0.08$ ) and manufacturer 2 ( $P = 0.41$ ) as seen in Table 3.2. Lactose was expected to remain in the continuous phase after treatment. Sepiolite physically entraps part of the continuous phase containing lactose and other soluble components as the sepiolite swells, but the sepiolite does not have an attractive force towards lactose (Guney et al., 2014).

Sepiolite did not change the ash content of the aqueous top layers from manufacturer 2 ( $P = 0.21$ ) as seen in Table 3.2. The top aqueous layers from manufacturer 1 treated with two grams of sepiolite per 100g GYW were significantly higher in ash than the top aqueous layers treated with the two other sepiolite treatments. However, the amount of ash did not increase by a notable degree and could be the result of additional sodium from the sodium hydroxide solution. Ash analysis by itself did not elude to any conclusive changes in the mineral content of the GYW from sepiolite addition.

The low amount of silicon from sepiolite present in the top aqueous layers did not have notable interference during atomic absorption and emission analysis. Calcium in the top aqueous layers from manufacturer 1 was not influenced by sepiolite addition ( $P = 0.12$ ) as seen in Table 3.2. The two grams of sepiolite per 100g of GYW treatment did show a slight significant increase in calcium content for the top aqueous layers from manufacturer 2. The increase in calcium was not observed with the four grams of sepiolite per 100g of GYW treatment for the

top aqueous layers from manufacturer 2. This trend could be similar the ash observations previously mentioned for the top aqueous layers from manufacturer 1. The pH and heat treatment alone remove about 75% of the calcium. Soluble calcium is not attracted to the sepiolite surface and remains in the continuous phase. Guney et al. (2014) used sepiolite to effectively remove heavy metals from the following salt solutions  $\text{CuCl}_2$ ,  $\text{ZnCl}_2$ , and  $\text{PbCl}_2$ . The large surface area and channels were contributed to the higher heavy metal adsorption but a specific mechanism was not identified. Soluble calcium could be competing against other components like proteins for adsorption sites on sepiolite.

The addition of sepiolite significantly decreased the phosphate content of the top aqueous layers for both manufacturers ( $P < 0.01$ ) as seen in Table 3.2. The addition of two grams of sepiolite per 100g of GYW significantly decreased the phosphates content in the top aqueous layers by about 80% for manufacturer 1 and 70% for manufacturer 2 compared to GYW from the manufacturer. Similarly, the addition of four grams of sepiolite per 100g of GYW significantly decreased the phosphates content by about 90% for manufacturer 1 and 77% for manufacturer 2 compared to GYW from the manufacturer. Dairy-derived phosphates can be present as  $\text{H}_2\text{PO}_4^-$  or  $\text{HPO}_4^{2-}$  or bound to calcium and magnesium (Fox and McSweeney, 1998).

The original sepiolite contains negligible phosphorus but sepiolite with GYW contains about 1.68% phosphorous as seen in Table 3.3. Therefore, phosphates could be adsorbing onto the sepiolite surface. According to Yin et al. (2011), effective phosphate absorbents normally contain high amounts of aluminum, iron, or calcium which readily adsorb phosphates or form stable phosphorus precipitates. Yin et al. (2011) observed the adsorption of phosphates from a phosphorus solution onto calcium-rich sepiolite material with over 20% CaO. The calcium-rich sepiolite material contained only 40 - 50% sepiolite with smectite, calcite, and dolomite as the

other main constituents. Phosphates effectively adsorbed onto the calcium-rich sepiolite material by forming calcium-bound phosphorus precipitations on the surface. The sepiolite in the present study contains only about 2.01% aluminum, 2.07% calcium, and 3.10% by weight iron as seen in Table 3.3. Therefore, another mechanism for phosphate adsorption is more likely.

Yan et al. (2010) suggested that anions including certain phosphates adsorb onto clay surfaces through ligand exchange and electrostatic interactions. Yan et al. (2010) observed an anion and OH<sup>-</sup> exchange reaction as the adsorption mechanism behind phosphates from a stock solution onto hydroxy-iron, hydroxy-aluminum, and hydroxy-iron-aluminum pillared bentonite clay minerals. Further research into the exact mechanism behind phosphate adsorption onto sepiolite surfaces is needed, but ligand exchange and electrostatic interactions are the most likely.

Sodium content was observed to see if the neutralization of the GYW with sodium hydroxide interfered with results from experimental treatment. The addition of sepiolite did not have an effect on the top aqueous layers from manufacturer 1 (P = 0.37) and manufacturer 2 (P = 0.83) as seen in Table 3.2. Therefore, the sodium remained in the continuous phase and did not interfere with other analysis.

The protein content in the top aqueous layers compared to the GYW from manufacturer 1 lowered about 45% without the addition of sepiolite and lowered about 60% after the addition of two or four grams of sepiolite per 100g of GYW. Similarly, for manufacturer 2 the addition of zero grams of sepiolite lowered the protein content in the top aqueous layers by about 25% compared to the GYW, while the addition of two or four grams of sepiolite per 100g of GYW lowered the protein content by about 45%. There was a significant difference in protein removal between the addition of zero and two grams of sepiolite per 100g of GYW treatments for both



manufacturers ( $P < 0.01$ ) as seen in Table 3.2. However, there was no significant difference in protein removal between the two and four grams of sepiolite per 100g of GYW treatments for both manufacturers. Electrostatic interactions between the sepiolite surface and the GYW proteins were suspected as the main mechanism for protein removal in the GYW by sepiolite.

Confocal microscopy, X-ray analysis, and SEM images were used to observe interactions between sepiolite and the whey proteins in the bottom sediment layers obtained after centrifugation of treated GYW with sepiolite added. The sepiolite surface without GYW appears rough with various tunnels and jagged edges as seen in Figure 3.4. Figure 3.5 shows particles with a more rounded morphology where the GYW proteins have adsorbed to sepiolite surfaces. The confocal microscopy image of sepiolite with GYW as seen in Figure 3.6a displays green fluorescent dye on the sepiolite surfaces indicating GYW protein attachment onto the sepiolite surface. Figure 3.6b shows a SEM image from the same area for comparison.

Yu et al. (2013) discussed possible mechanisms for interactions between clay minerals and proteins including cation exchange, cation bridge, hydrogen bonding, hydrophobic interactions, hydrophilic interactions, van der Waals forces, and electrostatic interactions. Barral et al. (2008) used a layered aluminosilicate clay mineral, kaolinite, to adsorb bovine serum albumin (BSA), beta-lactoglobulin ( $\beta$ -LG), and alpha-lactalbumin ( $\alpha$ -LA) from purified whey protein solutions. Maximum adsorption capacity was reached at the isoelectric point for each whey protein where 131mg  $\alpha$ -LA, 52mg BSA, and 77.5mg  $\beta$ -LG were adsorbed per gram of kaolinite. X-ray diffraction analysis of kaolinite with whey proteins revealed that protein adsorption takes place on the clay's external edges and surfaces. X-ray elemental component analysis of sepiolite with GYW in the present study showed about 11.79% carbon and 1.93% nitrogen by weight on the sepiolite surface compared to negligible nitrogen and about 1.39%

carbon with the original sepiolite as seen in Table 3.3. The appearance of additional carbon and nitrogen on the sepiolite surface indicate GYW protein attachment onto the sepiolite surface.

Barral et al. (2008) confirmed a lack of hydrogen bonding between whey proteins and the hydroxyl groups onto the surface of kaolinite's using Fourier transform infrared spectroscopy.

Barral et al. (2008) concluded that electrostatic interactions were the primary mechanism behind protein adsorption onto kaolinite surfaces. In addition, steric effects might also play a minor role. Similarly, electrostatic interactions are suspected to be the main mechanism for the adsorption of GYW proteins onto sepiolite.

The desorption of the GYW proteins was examined by washing GYW proteins adsorbed onto sepiolite with three washes of distilled water. Confocal microscopy of the washed sepiolite with GYW proteins showed similar results to the unwashed sepiolite with GYW proteins. With X-ray elemental component analysis, the washed sepiolite had a similar nitrogen and carbon concentration compared to sepiolite with GYW as seen in Table 3.3. Efficient desorption of the proteins was not accomplished because most of the proteins remained attached to the sepiolite surface after the distilled water wash. Barral et al. (2008) examined different eluents for desorbing whey proteins from a kaolinite surface: distilled water, 1M NaCl, polyethylene glycol, ethanol, ethanol with NaCl, and ethanol with sodium dodecyl sulfate (SDS). Only ethanol with SDS was determined to be an effective eluent for protein desorption. According to Yu et al. (2013), solution pH influences electrostatic interactions between proteins and clay surfaces by affecting the clay's surface charge and the protein's degree of ionization. Proteins have a maximum adsorption onto clay surfaces at their isoelectric point where the proteins experience the least amount of repulsive forces. Electrostatic interactions between clay surfaces and proteins

are weakened when the solution pH is greater than the isoelectric point. Therefore, basic conditions should favor the desorption of proteins from clay surfaces (Yu et al., 2013).

The sepiolite particles settled into the sediment layer along with the other insoluble components. The two grams of sepiolite per 100g of GWY treatment resulted in about a 0.5% decrease in TS for the top aqueous layers from both manufacturers ( $P < 0.01$ ) as seen in Table 3.2. Adding four grams of sepiolite per 100g of GWY from manufacturer 1 significantly decreased TS by about 1% in the top aqueous layers. There was no significant reduction in TS between the two and four grams of sepiolite per 100g of GYW treatments for manufacturer 2. The decrease in TS for the top aqueous layers is a result of the proteins and phosphates becoming attached to the sepiolite which separates into the bottom sediment layer. Similarly, heat treatment and pH neutralization of the GYW resulted in solids including ash and protein becoming insoluble and separating into the bottom sediment layer. Lactose can be recovered from GYW more efficiently using value-added processes including membrane filtration and evaporation if the ash and protein content is decreased. Proteins and ash contained within the sepiolite can also be recovered or repurposed as animal feed. The lactose rich top aqueous layer and the mineral and protein rich bottom sediment layer formed through pH neutralization, heating, and sepiolite addition are easier to add value to than non-treated GYW that exists in one single phase.

The continuous phase of the GYW becomes less opaque after the removal of the white insoluble calcium phosphates formed by the pH and heat treatment. The  $b^*$  value of the GYW continuous phase increased from 4.24 to 25.99 for manufacturer 1 and increased from 6.73 to 26.23 for manufacturer 2 after pH and heat treatment as seen in Table 3.1 and Table 3.2. Sepiolite treatment was effective at removing a majority of the yellow and green tint caused by the natural pigments in the GYW for both manufacturers. The addition of two grams of sepiolite

per 100g of GYW lowered the  $b^*$  in the top aqueous layers by about 70% ( $P < 0.01$ ) compared to the addition of no sepiolite for both manufacturers as seen in Table 3.2. However, there was no significant difference between the two and four grams of sepiolite per 100g of GYW treatments. The  $a^*$  for the GYW from both manufacturers lowered by about 90% after the addition of sepiolite ( $P < 0.01$ ) as seen in Table 3.2.

When the amount of sepiolite added was increased from two grams to four grams of sepiolite per 100g of GYW sepiolite the  $a^*$  significantly decreased about 50% further for GYW from manufacturer 1 and about 90% further for GYW from manufacturer 2. The  $L^*$  for the GYW from manufacturer 1 lowered about 20% after sepiolite treatment ( $P < 0.01$ ) but there was no significant difference in  $L^*$  when the amount of sepiolite increased from two to four grams per 100g of GYW. There was no definite pattern for  $L^*$  when sepiolite was added to the GYW from manufacturer 2. Other studies have confirmed that sepiolite is an effective adsorbent of aqueous dyes including Basic Astrazon yellow 7GL, methylene blue, and methyl violet dyes because of its large surface area (Tekbaş et al., 2009). Yellow pigment caused by annatto in whey powders and other value-added whey products used in baked goods, drinks, or other products can cause a lower perceived quality in the product by consumers (Kang et al., 2010). Sepiolite has been shown to effectively remove natural color that is undesirable to consumers from GYW.

## Conclusions

MFT and the addition of sepiolite were evaluated as possible methods for concentrating the valuable chemical components in GYW collected from two manufacturers. The pH and temperature parameters were confirmed as effective conditions to precipitate minerals. The MFT did not prove effective in aiding the removal of TS, ash, protein, minerals, or colored pigments from the GYW top aqueous layer for both manufacturers. Proper experimental parameters need to be further researched if MFT is to be a proposed treatment method for GYW. The addition of sepiolite combined with the temperature and pH conditions was able to increase the removal of TS, protein, phosphates, and color pigment. The adsorption of proteins onto the sepiolite surface was contributed to electrostatic effects, while the adsorption of dye pigments was contributed to sepiolite's large surface area. Although sepiolite did not concentrate all GYW minerals, applications for protein and color removal were discovered.

There is the opportunity to utilize layers formed by the addition of sepiolite, pH adjustment, and heat treatment of GYW. The top aqueous layer becomes lower in ash and protein content and thus can be more readily used with lactose recovery methods including membrane filtration. Sepiolite also removes the natural yellow pigment in GYW that is seen as a negative quality attribute by consumers. The bottom sediment layer can be used as an animal feed with higher concentrations of minerals and protein compared to GYW. Schell et al. (1993) fed bovines diets with sepiolite and found that the sepiolite aided in the health and weight gain of the animal. Methods need to be looked into for removing the GYW proteins from the surface of sepiolite to yield a cost effective whey protein concentrate. Clay minerals similar to sepiolite along with pH and temperature treatment have the ability to add value to GYW by isolating components and thus making it easier to recover or repurpose them.

### Acknowledgements for Chapter 3

I would like to thank Dairy Management Inc. (Rosemont, IL) as administered by Dairy Research Institute for their financial support along with Wilsa Inc. I also thank Ye Li, undergraduate student in Kansas State University department of statistics, and Dr. Leigh Murray, Director of the statistical consulting lab, for their statistical consulting services. I thank Cheryl Armendariz, Research Instructor at the Kansas State Nutrition Lab, for her help with mineral and protein analysis. I also thank Dr. Daniel Boyle from the Division of Biology at Kansas State University for his help with microscopy analysis. I thank the Nanotechnology Innovation Center of Kansas State for their help with the scanning electron microscopy images in the appendix. I finally thank my lab mates, Karthik Pandalaneni, Mary Hauser, Sara Menard, and Bingyi Li, and my major professor, Jayendra Amamcharla, for their support.

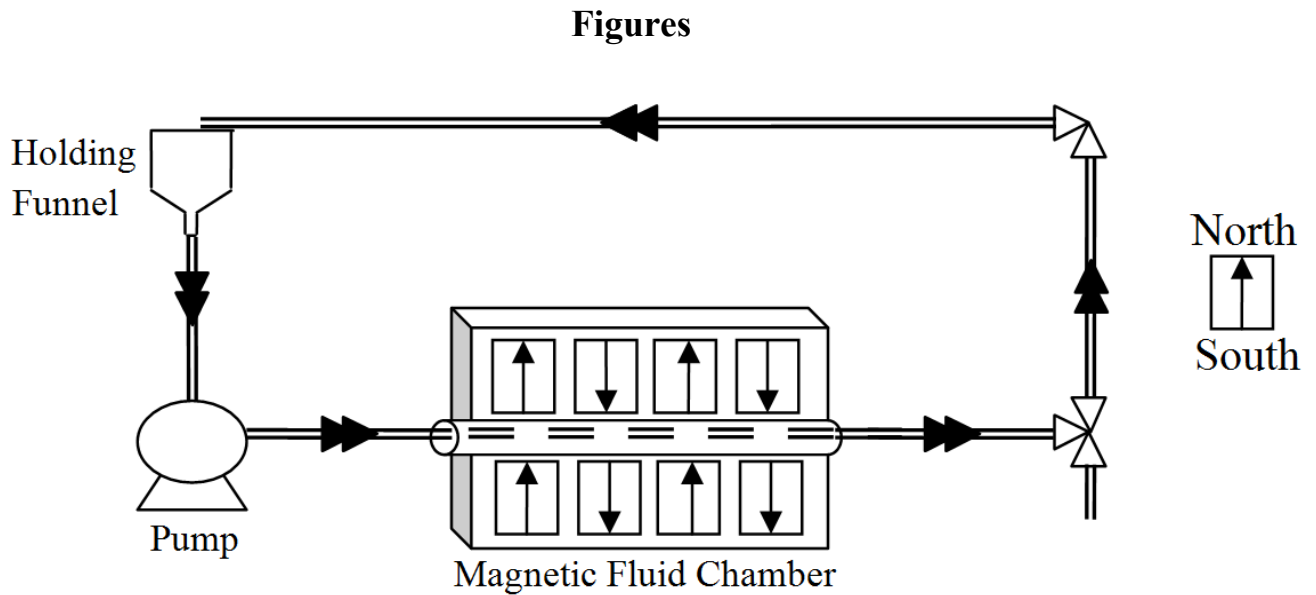


**Figure 3.1 Magnetic Fluid Treatment system design**

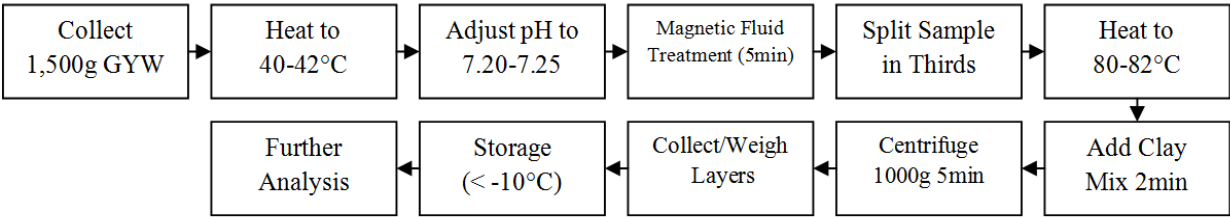



**Figure 3.2 Process flow diagram for treatment of Greek yogurt whey**

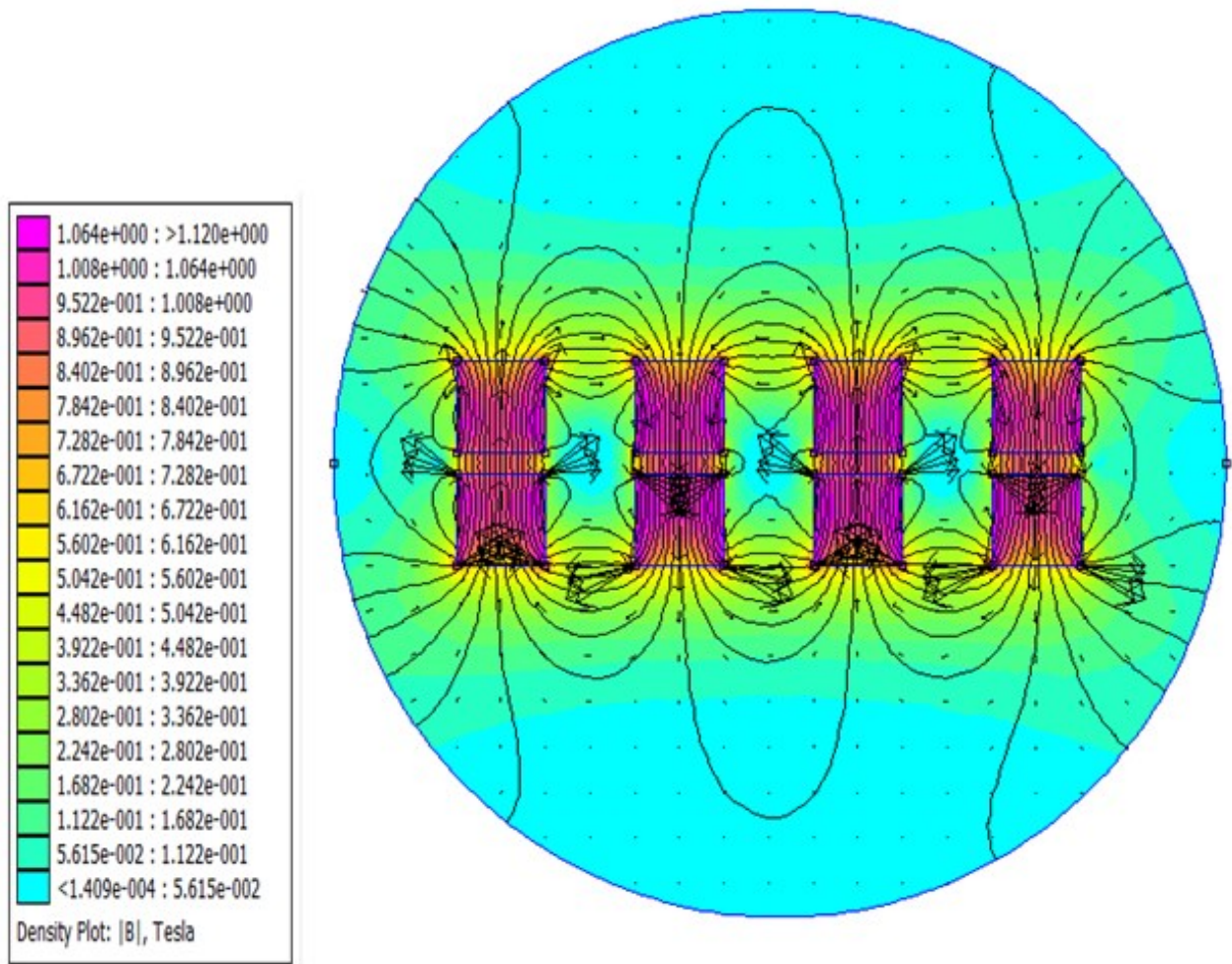
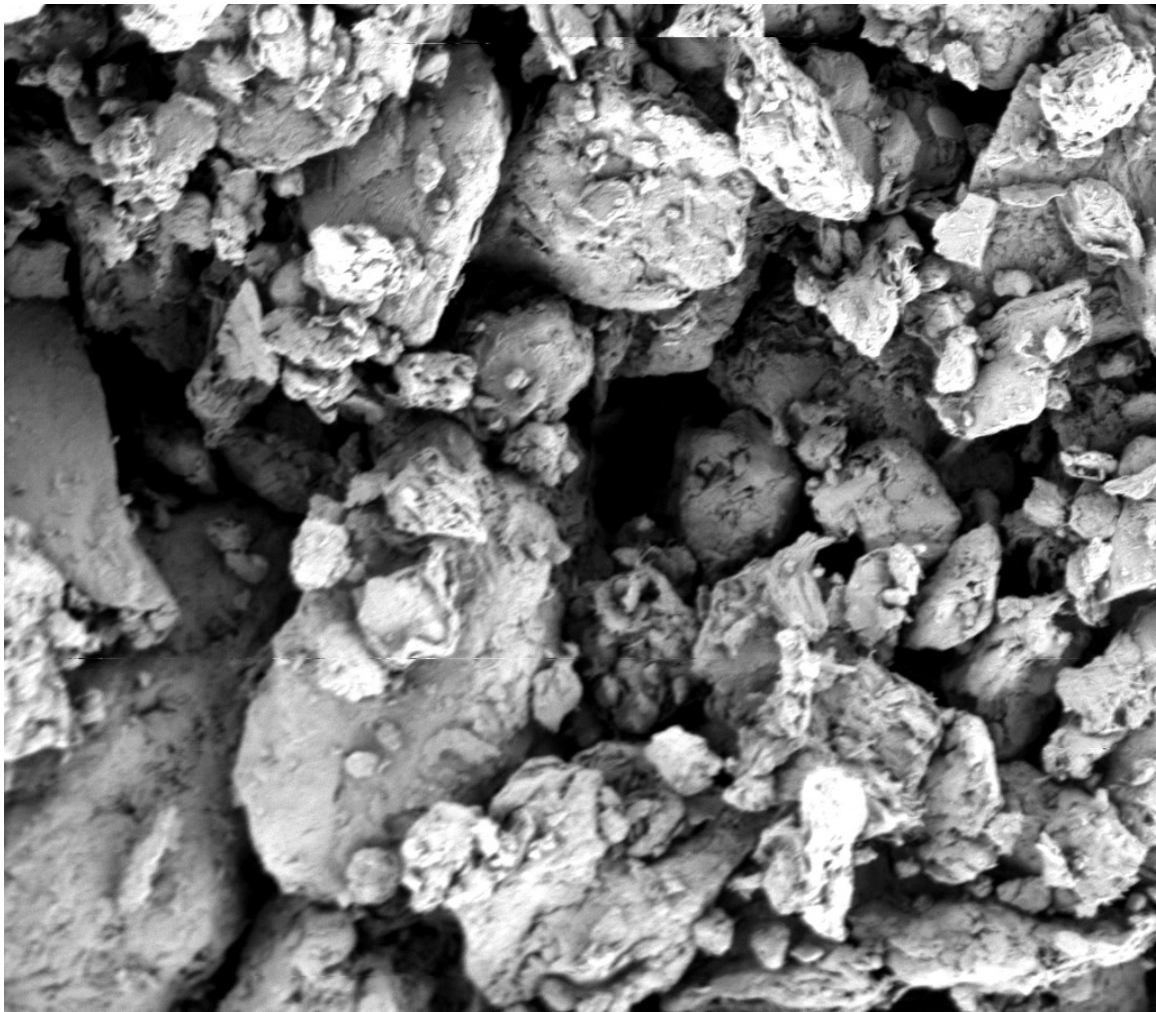


**Figure 3.3 Theoretical magnetic flux density plot for the Magnetic Fluid Treatment chamber**





	det	HV	WD	spot	HFW	mag	Landing E	← 10 μm →
vCD	5.00 kV	5.8 mm	4.0	59.7 μm	5 000 x	1.00 keV	Kansas State University	

**Figure 3.4 SEM image of sepiolite**

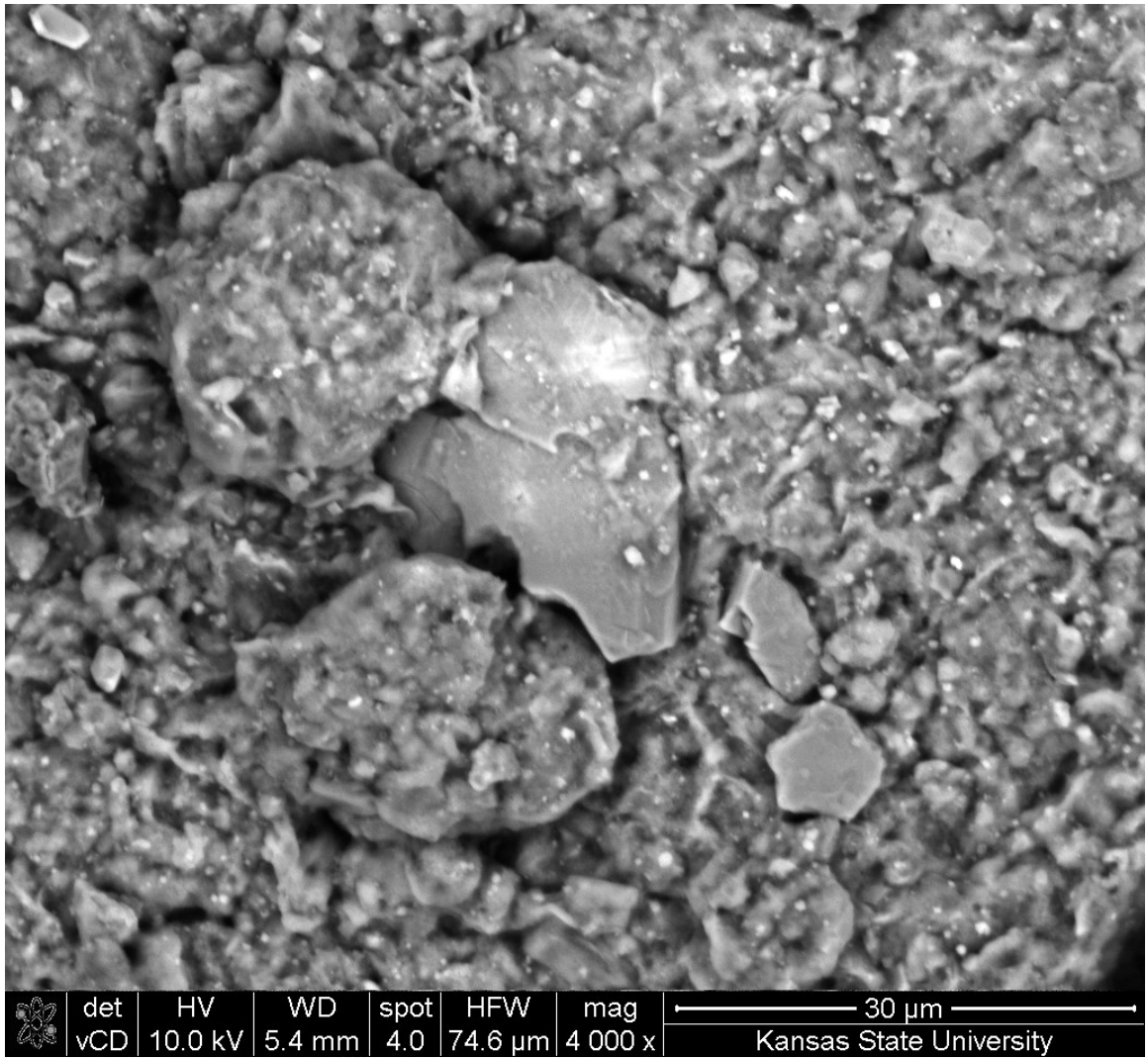
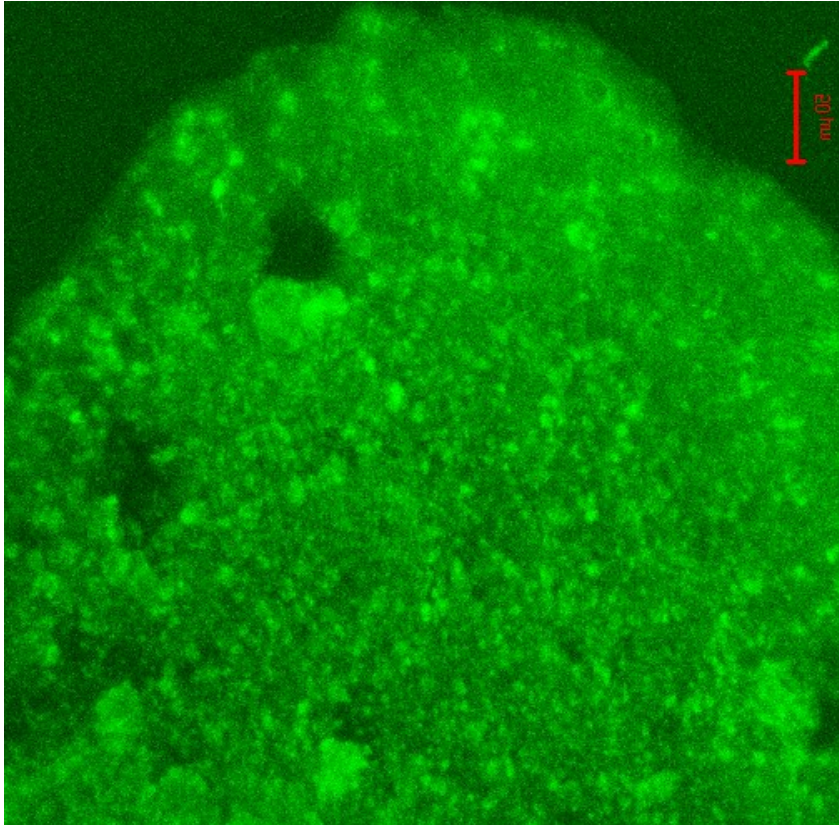


**Figure 3.5 SEM image of sepiolite with GYW**

a



b

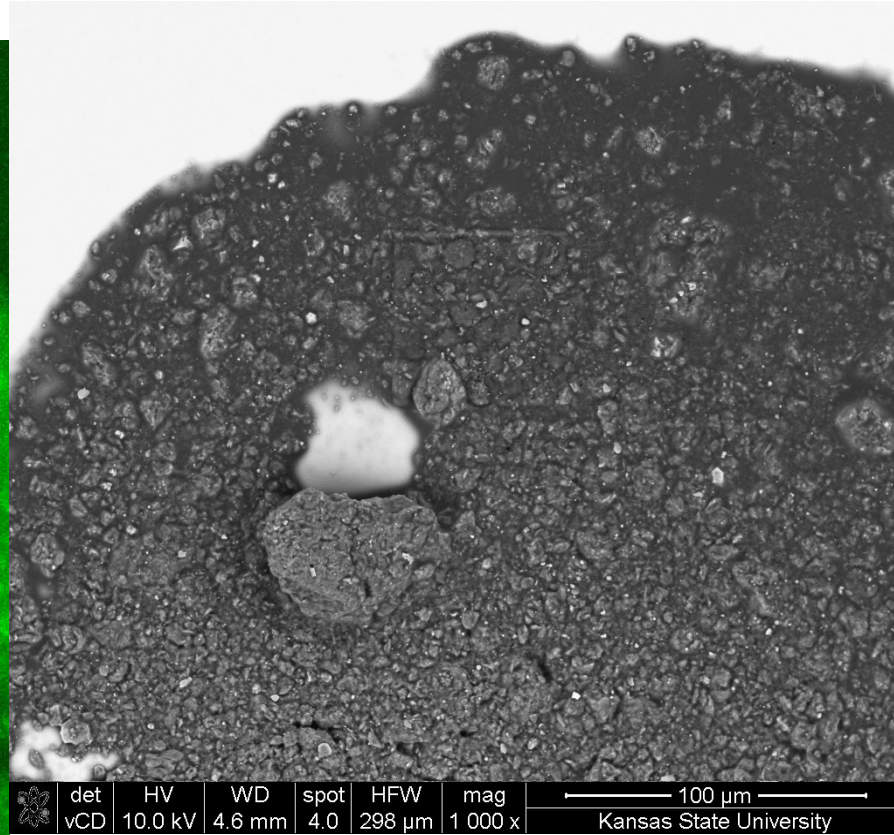


**Figure 3.6 Confocal microscopy image of dyed whey proteins on sepiolite surface (a) with corresponding SEM image (b) where green indicates the presence of proteins on the surface**

## Tables

**Table 3.1 Chemical composition of Greek yogurt whey collected from manufacturer 1 and manufacturer 2 (mean  $\pm$  standard deviation; n=2)**

Average		Manufacturer 1	Manufacturer 2
Chemical Property			
pH		4.27 $\pm$ 0.06 <sup>a</sup>	4.48 $\pm$ 0.02 <sup>b</sup>
TS (%)		6.02 $\pm$ 0.05 <sup>a</sup>	6.04 $\pm$ 0.04 <sup>a</sup>
Ash (%)		0.73 $\pm$ 0.01 <sup>a</sup>	0.73 $\pm$ 0.01 <sup>a</sup>
Protein (%)		0.27 $\pm$ 0.01 <sup>a</sup>	0.25 $\pm$ 0.02 <sup>a</sup>
Calcium (mg/100g)		126 $\pm$ 7 <sup>a</sup>	126 $\pm$ 12 <sup>a</sup>
Phosphates (mM)		6.88 $\pm$ 0.62 <sup>a</sup>	7.17 $\pm$ 0.41 <sup>a</sup>
Sodium (mg/100g)		39 $\pm$ 2 <sup>a</sup>	42 $\pm$ 1 <sup>a</sup>
Color	L*	13.21 $\pm$ 1.18 <sup>a</sup>	32.42 $\pm$ 1.00 <sup>b</sup>
	a*	-3.78 $\pm$ 0.06 <sup>a</sup>	-3.93 $\pm$ 0.53 <sup>a</sup>
	b*	4.24 $\pm$ 0.05 <sup>a</sup>	6.73 $\pm$ 0.430 <sup>b</sup>

<sup>a-b</sup>Means within a row with different superscripts differ (p< 0.05)

**Table 3.2 Effect of magnetic exposure and addition of sepiolite to the chemical composition of the top aqueous layers of Greek yogurt whey (mean ± standard deviation; n=2)**

Average Chemical Property	MFT <sup>1</sup>				Sepiolite Treatment <sup>1</sup>			
	Manufacturer	Magnetic Exposure	No Magnetic Exposure	MFT Effect P-Value	Grams of Sepiolite per 100g GYW			Sepiolite Effect P-Value
					0g	2g	4g	
TS (%)	1	5.78±0.04 <sup>a</sup>	5.79±0.05 <sup>a</sup>	0.12	5.82±0.03 <sup>c</sup>	5.78±0.04 <sup>d</sup>	5.76±0.04 <sup>c</sup>	<0.01
	2	5.81±0.06 <sup>a</sup>	5.81±0.06 <sup>a</sup>	0.95	5.84±0.04 <sup>c</sup>	5.80±0.07 <sup>d</sup>	5.79±0.05 <sup>d</sup>	<0.01
Ash (%)	1	0.759±0.008 <sup>a</sup>	0.759±0.006 <sup>a</sup>	0.78	0.759±0.006 <sup>c</sup>	0.762±0.007 <sup>d</sup>	0.755±0.005 <sup>c</sup>	<0.01
	2	0.730±0.008 <sup>a</sup>	0.729±0.005 <sup>a</sup>	0.66	0.759±0.006 <sup>c</sup>	0.762±0.007 <sup>d</sup>	0.755±0.005 <sup>c</sup>	0.21
Lactose (%)	1	3.53±0.09 <sup>a</sup>	3.50±0.11 <sup>a</sup>	0.31	3.57±0.10 <sup>c</sup>	3.48±0.10 <sup>c</sup>	3.50±0.1 <sup>c</sup>	0.08
	2	3.78±0.10 <sup>a</sup>	3.68±0.09 <sup>b</sup>	<0.01	3.73±0.12 <sup>c</sup>	3.75±0.13 <sup>c</sup>	3.70±0.07 <sup>c</sup>	0.41
Protein (%)	1	0.12±0.04 <sup>a</sup>	0.12±0.03 <sup>a</sup>	0.81	0.15±0.03 <sup>c</sup>	0.10±0.02 <sup>d</sup>	0.10±0.03 <sup>d</sup>	<0.01
	2	0.15±0.03 <sup>a</sup>	0.14±0.04 <sup>a</sup>	0.19	0.18±0.03 <sup>c</sup>	0.13±0.02 <sup>d</sup>	0.13±0.02 <sup>d</sup>	<0.01
Calcium (mg/100g)	1	29±2 <sup>a</sup>	28±2 <sup>a</sup>	0.25	28±2 <sup>c</sup>	29±2 <sup>c</sup>	29±1 <sup>c</sup>	0.12
	2	28±2 <sup>a</sup>	28±2 <sup>a</sup>	0.52	27±3 <sup>c</sup>	29±2 <sup>d</sup>	28±2 <sup>cd</sup>	0.03
Phosphates (mM)	1	1.40±0.65 <sup>a</sup>	1.30±0.65 <sup>a</sup>	0.19	2.05±0.35 <sup>c</sup>	1.27±0.31 <sup>d</sup>	0.72±0.34 <sup>e</sup>	<0.01
	2	2.28±0.64 <sup>a</sup>	2.18±0.65 <sup>a</sup>	0.20	2.97±0.25 <sup>c</sup>	2.12±0.27 <sup>d</sup>	1.61±0.39 <sup>e</sup>	<0.01
Sodium (mg/100g)	1	117±6 <sup>a</sup>	116±6 <sup>a</sup>	0.82	118±6 <sup>c</sup>	115±6 <sup>c</sup>	117±6 <sup>c</sup>	0.37
	2	138±4 <sup>a</sup>	139±6 <sup>a</sup>	0.91	138±7 <sup>c</sup>	139±3 <sup>c</sup>	139±3 <sup>c</sup>	0.83
L*	1	16.27±2.93 <sup>a</sup>	16.03±2.39 <sup>a</sup>	0.51	19.59±1.19 <sup>c</sup>	14.48±0.75 <sup>d</sup>	14.37±0.83 <sup>d</sup>	<0.01
	2	37.12±1.55 <sup>a</sup>	36.97±1.43 <sup>a</sup>	0.69	36.83±1.67 <sup>cd</sup>	36.47±1.12 <sup>c</sup>	37.83±1.32 <sup>d</sup>	0.03
A*	1	-1.42±1.74 <sup>a</sup>	-1.33±1.57 <sup>a</sup>	0.14	-3.63±0.33 <sup>c</sup>	-0.35±0.15 <sup>d</sup>	-0.15±0.16 <sup>e</sup>	<0.01
	2	-1.38±1.77 <sup>a</sup>	-1.40±1.77 <sup>a</sup>	0.78	-3.79±0.34 <sup>c</sup>	-0.35±0.21 <sup>d</sup>	-0.03±0.14 <sup>e</sup>	<0.01
B*	1	14.03±9.61 <sup>a</sup>	13.39±8.60 <sup>a</sup>	0.29	25.99±2.93 <sup>c</sup>	8.16±0.71 <sup>d</sup>	6.97±0.76 <sup>d</sup>	<0.01
	2	14.04±9.27 <sup>a</sup>	13.85±9.03 <sup>a</sup>	0.83	26.23±3.29 <sup>c</sup>	8.10±0.62 <sup>d</sup>	7.51±0.57 <sup>d</sup>	<0.01

<sup>a-b</sup>Means within a row with different superscripts differ (p<0.05)

<sup>c-e</sup>Means within a row with different superscripts differ (p<0.05)

<sup>1</sup>No interaction among magnetic and sepiolite treatments for all chemical properties (p>0.05)

**Table 3.3 X-ray elemental component analysis**

Element	Percent Weight Composition		
	Original sepiolite	4g sepiolite with	Washed 4g sepiolite with
		100g GYW bottom sediment layer	100g GYW bottom sediment layer <sup>1,2</sup>
C	1.39	11.79	9.83
N	0.00	1.93	2.01
O	54.05	48.03	36.54
F	2.30	1.79	1.35
Na	0.17	0.28	0.00
Mg	10.74	7.54	5.44
Al	2.01	1.62	0.90
Si	22.13	17.90	39.38
P	0.00	1.68	1.13
K	0.58	1.01	0.32
Ca	2.07	4.60	3.09
Fe	3.10	1.84	0.00
Ti	1.46	0.00	0.00

<sup>1</sup>Sample was stained with Fast Green FCF prior to X-ray component analysis

<sup>2</sup>Sample was washed three times with distilled water

## References

- Amamcharla, J.K., and L.E. Metzger. 2011. Development of a rapid method for the measurement of lactose in milk using a blood glucose biosensor. *J. Dairy Sci.* 94:4800–4809.
- Auty, M. a. E., M. Twomey, T.P. Guinee, and D.M. Mulvihill. 2001. Development and application of confocal scanning laser microscopy methods for studying the distribution of fat and protein in selected dairy products. *J. Dairy Res.* 68:417–427.
- Baltzis, K.B. 2009. The finite element method magnetics (FEMM) freeware package: may it serve as an educational tool in teaching electromagnetics? *Int. J. Inf. Educ. Technol.* 15:19–36.
- Barral, S., M.A. Villa-García, M. Rendueles, and M. Díaz. 2008. Interactions between whey proteins and kaolinite surfaces. *Acta Mater.* 56:2784–2790.
- Cai, R., H. Yang, J. He, and W. Zhu. 2009. The effects of magnetic fields on water molecular hydrogen bonds. *J. Mol. Struct.* 938:15–19.
- Chandan, R.C., and A. Kilara. 2010. *Dairy Ingredients for Food Processing*. Blackwell Publishing Ltd., Ames, Iowa. 64–68 pp.
- Corredig, M. 2009. *Dairy-Derived Ingredients: Food and Nutraceutical Uses*. 1st ed. Woodhead Publishing, Boca Raton, Cambridge. 110–112 pp.
- Desai, N.T., L. Shepard, and M.A. Drake. 2013. Sensory properties and drivers of liking for Greek yogurts. *J. Dairy Sci.* 96:7454–7466.
- Doğan, M., Y. Özdemir, and M. Alkan. 2007. Adsorption kinetics and mechanism of cationic methyl violet and methylene blue dyes onto sepiolite. *Dyes and Pigm.* 75:701–713.
- Fiske, C.H., and Y. Subbarow. 1925. The colorimetric determination of phosphorus. *J. Biol. Chem.* 66:375–400.
- Fox, P.F., and P.L.H. McSweeney. 1998. *Dairy Chemistry and Biochemistry*. Springer Science & Business Media. 261–262 pp.
- Guney, Y., B. Cetin, A.H. Aydilek, B.F. Tanyu, and S. Koparal. 2014. Utilization of sepiolite materials as a bottom liner material in solid waste landfills. *Waste Manag.* 34:112–124.
- Holysz, L., A. Szczes, and E. Chibowski. 2007. Effects of a static magnetic field on water and electrolyte solutions. *J. Colloid Interface Sci.* 316:996–1002.
- Kang, E.J., R.E. Campbell, E. Bastian, and M.A. Drake. 2010. Invited review: Annatto usage and bleaching in dairy foods. *J. Dairy Sci.* 93:3891–3901.
- Keller, A.K., inventor. 2015. Process and system for drying acid whey. Proliant Dairy Inc., assignee. US Pat. App. No. 13/974,718.

- Lipus, L.C., and D. Dobersek. 2007. Influence of magnetic field on the aragonite precipitation. *Chem. Eng. Sci.* 62:2089–2095.
- Özcan, A., E.M. Öncü, and A.S. Özcan. 2006. Kinetics, isotherm and thermodynamic studies of adsorption of Acid Blue 193 from aqueous solutions onto natural sepiolite. *Colloids Surf. A Physicochem. Eng. Asp.* 277:90–97.
- Schell, T.C., M.D. Lindemann, E.T. Kornegay, D.J. Blodgett, and J.A. Doerr. 1993. Effectiveness of different types of clay for reducing the detrimental effects of aflatoxin-contaminated diets on performance and serum profiles of weanling pigs. *J. Anim. Sci.* 71:1226–1231.
- Strazisar, J., S. Knez, and S. Kobe. 2001. The influence of the magnetic field on the zeta potential of precipitated calcium carbonate. *Part. Part. Syst. Charact.* 18:278–285.
- Tekbaş, M., N. Bektaş, and H.C. Yatmaz. 2009. Adsorption studies of aqueous basic dye solutions using sepiolite. *Desalination.* 249:205–211.
- Wehr, M., P. and J.F. Frank. 2004. *Standard Methods for the Examination of Dairy Products.* 17th edition. American Public Health Association, Washington, DC. 380-384, 442–459 pp.
- Yan, L., Y. Xu, H. Yu, X. Xin, Q. Wei, and B. Du. 2010. Adsorption of phosphate from aqueous solution by hydroxy-aluminum, hydroxy-iron and hydroxy-iron–aluminum pillared bentonites. *J. Hazard. Mater.* 179:244–250.
- Yin, H., Y. Yun, Y. Zhang, and C. Fan. 2011. Phosphate removal from wastewaters by a naturally occurring, calcium-rich sepiolite. *J. Hazard. Mater.* 198:362–369.
- Yu, W.H., N. Li, D.S. Tong, C.H. Zhou, C.X. (Cynthia) Lin, and C.Y. Xu. 2013. Adsorption of proteins and nucleic acids on clay minerals and their interactions: A review. *Appl. Clay Sci.* 80–81:443–452.
- Zucchetti, S., and G. Contarini. 1993. AAS determination of calcium, sodium, and potassium in dairy products using TCA for extraction. *Atomic spectroscopy.* 14:60–64.



## Appendix A - Image of Magnetic Fluid Treatment System from Chapter 3



Figure A.1 Image of Magnetic Fluid Treatment System from Chapter 3

# Appendix B - Additional Theoretical Magnetic Field Design for Chapter 3

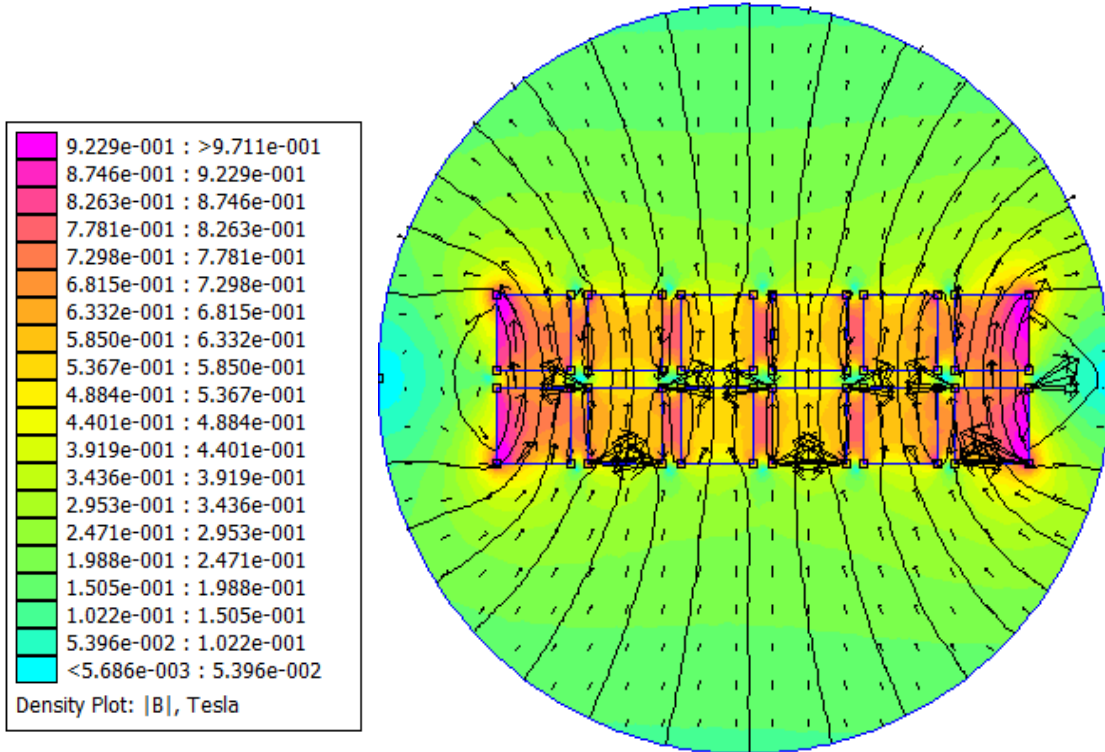


Figure B.1 Theoretical Magnetic Flux Density Plot for Constant Magnetic Pair Orientation

## Appendix C - Raw Data and SAS Code for Manufacturer 1 for Chapter 3

```

data yogurt;
input ID$ Magnet$ Clay$ TS Ash Lactose Aveb Protein Batch$ P Ca Na AveL
AveA;
datalines;
1A Yes 0g/100g 5.848 0.759 3.539 28.450 0.180 a 2.521 0.027
0.161 20.683 -3.820
2A Yes 2g/100g 5.797 0.762 3.655 8.800 0.113 a 1.749 0.029 0.155
15.164 -0.270
3A Yes 4g/100g 5.794 0.757 3.636 7.190 0.109 a 1.020 0.031 0.165
14.534 0.043
4A No 0g/100g 5.855 0.762 3.745 19.427 0.172 a 2.483 0.027
0.161 16.680 -3.287
5A No 2g/100g 5.817 0.759 3.432 7.407 0.109 a 1.671 0.031 0.153
13.744 -0.360
6A No 4g/100g 5.778 0.761 3.566 6.710 0.109 a 1.239 0.030 0.166
14.296 -0.080
7A Yes 0g/100g 5.843 0.762 3.492 22.480 0.169 a 2.307 0.029
0.166 18.617 -3.377
8A Yes 2g/100g 5.830 0.773 3.472 6.567 0.112 a 1.551 0.032 0.158
13.090 -0.153
9A Yes 4g/100g 5.806 0.756 3.553 5.903 0.100 a 0.891 0.029 0.162
13.153 -0.210
10A No 0g/100g 5.853 0.766 3.483 23.960 0.153 a 2.424 0.028
0.158 19.072 -3.250
11A No 2g/100g 5.830 0.769 3.547 7.770 0.098 a 1.505 0.029 0.154
14.108 -0.193
12A No 4g/100g 5.822 0.757 3.464 7.670 0.086 a 0.916 0.028 0.157
14.710 -0.053
1B Yes 0g/100g 5.815 0.749 3.522 28.540 0.131 b 2.419 0.029
0.159 20.847 -3.743
2B Yes 2g/100g 5.797 0.758 3.512 8.513 0.075 b 1.496 0.029 0.156
14.713 -0.323
3B Yes 4g/100g 5.742 0.750 3.579 7.553 0.069 b 1.098 0.030 0.157
15.524 -0.177
4B No 0g/100g 5.848 0.754 3.594 24.450 0.126 b 1.736 0.026
0.167 18.790 -3.110
5B No 2g/100g 5.825 0.755 3.539 8.733 0.076 b 1.077 0.027 0.160
15.184 -0.250
6B No 4g/100g 5.776 0.752 3.604 5.737 0.071 b 0.766 0.029 0.162
13.436 0.207
7B Yes 0g/100g 5.802 0.746 3.674 25.563 0.122 b 1.891 0.027
0.162 19.519 -3.717
8B Yes 2g/100g 5.783 0.759 3.553 8.153 0.065 b 1.336 0.026 0.163
14.966 -0.333
9B Yes 4g/100g 5.745 0.746 3.408 7.627 0.050 b 0.781 0.028 0.160
15.291 -0.147
10B No 0g/100g 5.822 0.754 3.600 26.797 0.089 b 1.839 0.028
0.162 19.821 -3.467
11B No 2g/100g 5.750 0.750 3.446 8.197 0.118 b 0.843 0.028 0.162
14.834 -0.643

```

12B	No	4g/100g	5.796	0.754	3.380	5.970	0.112	b	0.663	0.027	0.159
			13.279	-0.337							
1C	Yes	0g/100g	5.788	0.764	3.666	29.123	0.174	c	1.725	0.032	0.032
			0.032	20.701	-4.213						
2C	Yes	2g/100g	5.756	0.763	3.445	7.973	0.142	c	0.918	0.030	0.030
			13.777	-0.480							
3C	Yes	4g/100g	5.723	0.764	3.343	6.680	0.113	c	0.420	0.030	0.030
			13.827	-0.323							
4C	No	0g/100g	5.785	0.763	3.528	27.893	0.145	c	1.694	0.028	0.028
			0.028	20.233	-3.880						
5C	No	2g/100g	5.753	0.761	3.266	9.257	0.114	c	1.070	0.032	0.032
			15.563	-0.483							
6C	No	4g/100g	5.711	0.749	3.421	7.647	0.182	c	0.187	0.027	0.027
			14.937	-0.367							
7C	Yes	0g/100g	5.765	0.760	3.596	28.163	0.167	c	1.681	0.026	0.026
			0.026	20.407	-3.973						
8C	Yes	2g/100g	5.722	0.775	3.427	8.030	0.106	c	1.122	0.029	0.029
			13.850	-0.243							
9C	Yes	4g/100g	5.717	0.758	3.479	7.133	0.095	c	0.232	0.029	0.029
			14.116	-0.163							
10C	No	0g/100g	5.785	0.764	3.385	26.980	0.166	c	1.874	0.028	0.028
			0.028	19.759	-3.757						
11C	No	2g/100g	5.734	0.765	3.437	8.517	0.103	c	0.946	0.029	0.029
			14.760	-0.507							
12C	No	4g/100g	5.711	0.759	3.530	7.853	0.094	c	0.397	0.029	0.029
			15.380	-0.180							

```

;
run;

proc print data=yogurt;
run;

/*Lactose*/
proc mixed data=yogurt;
class Magnet Clay Batch;
model Lactose= Magnet Clay Clay*Magnet ;

random Batch Batch*Magnet*Clay;

lsmeans Magnet Clay Clay*Magnet /cl;

/*Object1 difference between three clay treatments for Lactose*/

estimate 'obj1_1 (0g vs 2g)' Clay 1 -1 0 ;
estimate 'obj1_2 (0g vs 4g)' Clay 1 0 -1 ;
estimate 'obj1_3 (2g vs 4g)' Clay 0 1 -1 ;

run;

/*TS*/
proc mixed data=yogurt;
class Magnet Clay Batch;
model TS= Magnet Clay Clay*Magnet ;

random Batch Batch*Magnet*Clay;

```

```

lsmeans Magnet Clay Clay*Magnet;

      /*Object2 difference between three clay treatments for TS*/

estimate  'obj2_1 (0g vs 2g)' Clay 1 -1 0 ;
estimate  'obj2_2 (0g vs 4g)' Clay 1 0 -1 ;
estimate  'obj2_3 (2g vs 4g)' Clay 0 1 -1 ;

run;

/*Ash*/
proc mixed data=yogurt;
class Magnet Clay Batch;
model Ash= Magnet Clay Clay*Magnet ;

random Batch Batch*Magnet*Clay;

lsmeans Magnet Clay Clay*Magnet;

      /*Object3 difference between three clay treatments for Ash*/

estimate  'obj3_1 (0g vs 2g)' Clay 1 -1 0 ;
estimate  'obj3_2 (0g vs 4g)' Clay 1 0 -1 ;
estimate  'obj3_3 (2g vs 4g)' Clay 0 1 -1 ;

run;

/*Color_b*/
proc mixed data=yogurt;
class Magnet Clay Batch;
model aveb= Magnet Clay Clay*Magnet ;

random Batch Batch*Magnet*Clay;

lsmeans Magnet Clay Clay*Magnet;

      /*Object2 difference between three clay treatments for TS*/

estimate  'obj2_1 (0g vs 2g)' Clay 1 -1 0 ;
estimate  'obj2_2 (0g vs 4g)' Clay 1 0 -1 ;
estimate  'obj2_3 (2g vs 4g)' Clay 0 1 -1 ;

run;

/*Protein*/
proc mixed data=yogurt;
class Magnet Clay Batch;
model Protein= Magnet Clay Clay*Magnet ;

random Batch Batch*Magnet*Clay;

lsmeans Magnet Clay Clay*Magnet ;

      /*Object4 difference between three clay treatments for Protein*/

```

```

estimate 'obj4_1 (0g vs 2g)' Clay 1 -1 0 ;
estimate 'obj4_2 (0g vs 4g)' Clay 1 0 -1 ;
estimate 'obj4_3 (2g vs 4g)' Clay 0 1 -1 ;

run;

/*Phosphate*/
proc mixed data=yogurt;
class Magnet Clay Batch;
model P= Magnet Clay Clay*Magnet ;

random Batch Batch*Magnet*Clay;

lsmeans Magnet Clay Clay*Magnet ;

/*Object4 difference between three clay treatments for Phosphate*/

estimate 'obj4_1 (0g vs 2g)' Clay 1 -1 0 ;
estimate 'obj4_2 (0g vs 4g)' Clay 1 0 -1 ;
estimate 'obj4_3 (2g vs 4g)' Clay 0 1 -1 ;

run;

/*Calcium*/
proc mixed data=yogurt;
class Magnet Clay Batch;
model Ca= Magnet Clay Clay*Magnet ;

random Batch Batch*Magnet*Clay;

lsmeans Magnet Clay Clay*Magnet ;

/*Object4 difference between three clay treatments for Ca*/

estimate 'obj4_1 (0g vs 2g)' Clay 1 -1 0 ;
estimate 'obj4_2 (0g vs 4g)' Clay 1 0 -1 ;
estimate 'obj4_3 (2g vs 4g)' Clay 0 1 -1 ;

run;

/*Sodium*/
proc mixed data=yogurt;
class Magnet Clay Batch;
model Na= Magnet Clay Clay*Magnet ;

random Batch Batch*Magnet*Clay;

lsmeans Magnet Clay Clay*Magnet ;

/*Object4 difference between three clay treatments for Na*/

estimate 'obj4_1 (0g vs 2g)' Clay 1 -1 0 ;
estimate 'obj4_2 (0g vs 4g)' Clay 1 0 -1 ;
estimate 'obj4_3 (2g vs 4g)' Clay 0 1 -1 ;

```

```

run;
/*Color_L*/
proc mixed data=yogurt;
class Magnet Clay Batch;
model AveL= Magnet Clay Clay*Magnet ;

random Batch Batch*Magnet*Clay;

lsmeans Magnet Clay Clay*Magnet ;

/*Object4 difference between three clay treatments for L*/

estimate 'obj4_1 (0g vs 2g)' Clay 1 -1 0 ;
estimate 'obj4_2 (0g vs 4g)' Clay 1 0 -1 ;
estimate 'obj4_3 (2g vs 4g)' Clay 0 1 -1 ;

run;
/*Color_A*/
proc mixed data=yogurt;
class Magnet Clay Batch;
model AveA= Magnet Clay Clay*Magnet ;

random Batch Batch*Magnet*Clay;

lsmeans Magnet Clay Clay*Magnet ;

/*Object4 difference between three clay treatments for A*/

estimate 'obj4_1 (0g vs 2g)' Clay 1 -1 0 ;
estimate 'obj4_2 (0g vs 4g)' Clay 1 0 -1 ;
estimate 'obj4_3 (2g vs 4g)' Clay 0 1 -1 ;

run;
/*Summary*/
proc summary data=yogurt;

var TS Ash Lactose Aveb Protein P Ca Na AveL AveA;
title "Summary for magnet";
class magnet;
output out=summary_magnet;
run;

proc print data=summary_magnet;
run;

proc summary data=yogurt;
title "Summary for clay";
var TS Ash Lactose Aveb Protein P Ca Na AveL AveA;
class clay;
output out=summary_clay;

```

```
run;  
  
proc print data=summary_clay;  
run;
```



## Appendix D - Raw Data and SAS Code for Manufacturer 2 for Chapter 3

```

data yogurt;
input ID$ Magnet$ Clay$ TS Ash Lactose Aveb Protein Batch$ P Ca Na AveL
AveA;
datalines;
1A Yes 0g/100g 24.267 3.023 3.789 26.513 0.880 a 3.038
0.095 0.573 37.440 -3.417
2A Yes 2g/100g 23.185 2.956 3.725 8.077 0.633 a 2.530 0.120
0.529 36.047 -0.227
3A Yes 4g/100g 22.023 2.781 3.777 7.663 0.675 a 2.190 0.108
0.519 38.713 -0.140
4A No 0g/100g 24.315 3.054 3.489 23.420 0.966 a 3.231
0.117 0.572 37.010 -3.823
5A No 2g/100g 23.205 2.955 3.549 7.537 0.483 a 2.539 0.127
0.560 35.970 -0.477
6A No 4g/100g 21.912 2.758 3.650 7.817 0.471 a 1.907 0.108
0.517 37.040 -0.207
7A Yes 0g/100g 24.081 3.030 3.759 24.647 0.840 a 3.117
0.141 0.547 35.623 -3.800
8A Yes 2g/100g 22.950 2.902 3.664 8.770 0.599 a 2.042 0.114
0.548 37.027 -0.443
9A Yes 4g/100g 21.871 2.768 3.633 7.293 0.508 a 1.661 0.110
0.509 37.463 0.027
10A No 0g/100g 24.288 3.080 3.660 22.970 0.814 a 3.149
0.121 0.577 33.833 -3.567
11A No 2g/100g 22.937 2.901 3.591 8.420 0.482 a 1.998 0.132
0.537 35.983 -0.517
12A No 4g/100g 21.812 2.746 3.592 7.700 0.445 a 1.581 0.112
0.515 38.490 0.017
1B Yes 0g/100g 24.578 3.112 3.775 22.017 0.687 b 3.203
0.116 0.594 36.357 -3.537
2B Yes 2g/100g 23.429 2.926 3.839 8.023 0.569 b 2.251 0.117
0.571 36.433 -0.303
3B Yes 4g/100g 22.246 2.775 3.756 7.437 0.539 b 1.763 0.106
0.542 38.290 0.173
4B No 0g/100g 24.513 3.060 3.735 23.200 0.698 b 3.025
0.111 0.584 36.637 -3.517
5B No 2g/100g 23.111 2.936 3.848 7.060 0.403 b 2.318 0.114
0.571 36.817 0.073
6B No 4g/100g 22.383 2.818 3.694 8.680 0.462 b 1.845 0.106
0.535 38.017 -0.077
7B Yes 0g/100g 24.375 3.095 3.769 23.980 0.688 b 3.127
0.119 0.591 34.580 -3.280
8B Yes 2g/100g 23.085 2.979 3.796 8.137 0.517 b 2.179 0.118
0.556 34.647 -0.140
9B Yes 4g/100g 22.104 2.777 3.790 6.467 0.401 b 1.871 0.109
0.536 34.990 0.120
10B No 0g/100g 24.310 3.035 3.696 27.547 0.645 b 2.657
0.110 0.600 35.977 -3.897
11B No 2g/100g 23.400 2.946 3.738 6.997 0.454 b 2.144 0.113
0.561 35.250 -0.313

```

12B	No	4g/100g	22.322	2.839	3.683	7.003	0.407	b	1.599	0.113
		0.543	35.893	0.213						
1C	Yes	0g/100g	24.833	3.069	3.852	30.243		0.578	c	2.635
		0.109	0.597	38.610	-4.187					
2C	Yes	2g/100g	23.496	2.935	4.067	8.770	0.574	c	1.788	0.117
		0.567	39.173	-0.393						
3C	Yes	4g/100g	22.377	2.766	3.772	7.707	0.494	c	0.850	0.096
		0.530	39.203	-0.057						
4C	No	0g/100g	24.539	3.074	3.797	30.100		0.794	c	2.924
		0.100	0.599	38.987	-4.083					
5C	No	2g/100g	23.718	2.933	3.690	8.340	0.559	c	1.723	0.118
		0.569	37.197	-0.250						
6C	No	4g/100g	22.375	2.721	3.739	7.953	0.496	c	1.006	0.094
		0.541	38.967	-0.233						
7C	Yes	0g/100g	24.922	3.084	3.902	31.343		0.811	c	2.999
		0.110	0.604	39.073	-4.390					
8C	Yes	2g/100g	23.131	2.892	3.718	8.797	0.538	c	2.096	0.113
		0.550	36.780	-0.753						
9C	Yes	4g/100g	22.749	2.885	3.624	6.863	0.496	c	1.755	0.116
		0.532	37.690	-0.063						
10C	No	0g/100g	24.651	3.080	3.555	28.817		0.821	c	2.471
		0.095	0.495	37.773	-3.993					
11C	No	2g/100g	23.655	2.971	3.748	8.237	0.541	c	1.832	0.111
		0.571	36.347	-0.433						
12C	No	4g/100g	22.719	2.838	3.695	7.533	0.507	c	1.248	0.111
		0.566	39.250	-0.130						

```

;
run;

proc print data=yogurt;
run;

/*Lactose*/
proc mixed data=yogurt;
class Magnet Clay Batch;
model Lactose= Magnet Clay Clay*Magnet ;

random Batch Batch*Magnet*Clay;

lsmeans Magnet Clay Clay*Magnet /cl;

/*Object1 difference between three clay treatments for Lactose*/

estimate 'obj1_1 (0g vs 2g)' Clay 1 -1 0 ;
estimate 'obj1_2 (0g vs 4g)' Clay 1 0 -1 ;
estimate 'obj1_3 (2g vs 4g)' Clay 0 1 -1 ;

run;

/*TS*/
proc mixed data=yogurt;
class Magnet Clay Batch;
model TS= Magnet Clay Clay*Magnet ;

random Batch Batch*Magnet*Clay;

```

```

lsmeans Magnet Clay Clay*Magnet;

    /*Object2 difference between three clay treatments for TS*/

estimate  'obj2_1 (0g vs 2g)' Clay 1 -1 0 ;
estimate  'obj2_2 (0g vs 4g)' Clay 1 0 -1 ;
estimate  'obj2_3 (2g vs 4g)' Clay 0 1 -1 ;

run;

/*Ash*/
proc mixed data=yogurt;
class Magnet Clay Batch;
model Ash= Magnet Clay Clay*Magnet ;

random Batch Batch*Magnet*Clay;

lsmeans Magnet Clay Clay*Magnet;

    /*Object3 difference between three clay treatments for Ash*/

estimate  'obj3_1 (0g vs 2g)' Clay 1 -1 0 ;
estimate  'obj3_2 (0g vs 4g)' Clay 1 0 -1 ;
estimate  'obj3_3 (2g vs 4g)' Clay 0 1 -1 ;

run;

/*Color_b*/
proc mixed data=yogurt;
class Magnet Clay Batch;
model aveb= Magnet Clay Clay*Magnet ;

random Batch Batch*Magnet*Clay;

lsmeans Magnet Clay Clay*Magnet;

    /*Object2 difference between three clay treatments for TS*/

estimate  'obj2_1 (0g vs 2g)' Clay 1 -1 0 ;
estimate  'obj2_2 (0g vs 4g)' Clay 1 0 -1 ;
estimate  'obj2_3 (2g vs 4g)' Clay 0 1 -1 ;

run;

/*Protein*/
proc mixed data=yogurt;
class Magnet Clay Batch;
model Protein= Magnet Clay Clay*Magnet ;

random Batch Batch*Magnet*Clay;

lsmeans Magnet Clay Clay*Magnet ;

    /*Object4 difference between three clay treatments for Protein*/

```

```

estimate 'obj4_1 (0g vs 2g)' Clay 1 -1 0 ;
estimate 'obj4_2 (0g vs 4g)' Clay 1 0 -1 ;
estimate 'obj4_3 (2g vs 4g)' Clay 0 1 -1 ;

run;

/*Phosphate*/
proc mixed data=yogurt;
class Magnet Clay Batch;
model P= Magnet Clay Clay*Magnet ;

random Batch Batch*Magnet*Clay;

lsmeans Magnet Clay Clay*Magnet ;

/*Object4 difference between three clay treatments for Phosphate*/

estimate 'obj4_1 (0g vs 2g)' Clay 1 -1 0 ;
estimate 'obj4_2 (0g vs 4g)' Clay 1 0 -1 ;
estimate 'obj4_3 (2g vs 4g)' Clay 0 1 -1 ;

run;

/*Calcium*/
proc mixed data=yogurt;
class Magnet Clay Batch;
model Ca= Magnet Clay Clay*Magnet ;

random Batch Batch*Magnet*Clay;

lsmeans Magnet Clay Clay*Magnet ;

/*Object4 difference between three clay treatments for Ca*/

estimate 'obj4_1 (0g vs 2g)' Clay 1 -1 0 ;
estimate 'obj4_2 (0g vs 4g)' Clay 1 0 -1 ;
estimate 'obj4_3 (2g vs 4g)' Clay 0 1 -1 ;

run;

/*Sodium*/
proc mixed data=yogurt;
class Magnet Clay Batch;
model Na= Magnet Clay Clay*Magnet ;

random Batch Batch*Magnet*Clay;

lsmeans Magnet Clay Clay*Magnet ;

/*Object4 difference between three clay treatments for Na*/

estimate 'obj4_1 (0g vs 2g)' Clay 1 -1 0 ;
estimate 'obj4_2 (0g vs 4g)' Clay 1 0 -1 ;
estimate 'obj4_3 (2g vs 4g)' Clay 0 1 -1 ;

```

```

run;
/*Color_L*/
proc mixed data=yogurt;
class Magnet Clay Batch;
model AveL= Magnet Clay Clay*Magnet ;

random Batch Batch*Magnet*Clay;

lsmeans Magnet Clay Clay*Magnet ;

/*Object4 difference between three clay treatments for L*/

estimate 'obj4_1 (0g vs 2g)' Clay 1 -1 0 ;
estimate 'obj4_2 (0g vs 4g)' Clay 1 0 -1 ;
estimate 'obj4_3 (2g vs 4g)' Clay 0 1 -1 ;

run;
/*Color_A*/
proc mixed data=yogurt;
class Magnet Clay Batch;
model AveA= Magnet Clay Clay*Magnet ;

random Batch Batch*Magnet*Clay;

lsmeans Magnet Clay Clay*Magnet ;

/*Object4 difference between three clay treatments for A*/

estimate 'obj4_1 (0g vs 2g)' Clay 1 -1 0 ;
estimate 'obj4_2 (0g vs 4g)' Clay 1 0 -1 ;
estimate 'obj4_3 (2g vs 4g)' Clay 0 1 -1 ;

run;
/*Summary*/

proc summary data=yogurt;

var TS Ash Lactose Aveb Protein P Ca Na AveL AveA;
title "Summary for magnet";
class magnet;
output out=summary_magnet;
run;

proc print data=summary_magnet;
run;

proc summary data=yogurt;
title "Summary for clay";
var TS Ash Lactose Aveb Protein P Ca Na AveL AveA;
class clay;
output out=summary_clay;

```

```
run;  
  
proc print data=summary_clay;  
run;
```

## **Appendix E - Additional SEM Images for Chapter 3**

### **Materials and Methods for the Following SEM Images**

A scanning electron microscope (S-3500N SEM, Hitachi, Ltd., Tokyo, Japan) was used to observe the surface morphology of the two and four grams of sepiolite per 100g Greek yogurt whey sediment layers. The samples were dried at 40°C for 12h and sputtering coated with 15-20nm of gold palladium using a fine ion coat sputter (Denton Desk II Vacuum Sputter Coater, Denton Vacuum, LLC., Moorestown, NJ). The samples were then observed under SEM with 15kV accelerating voltage.

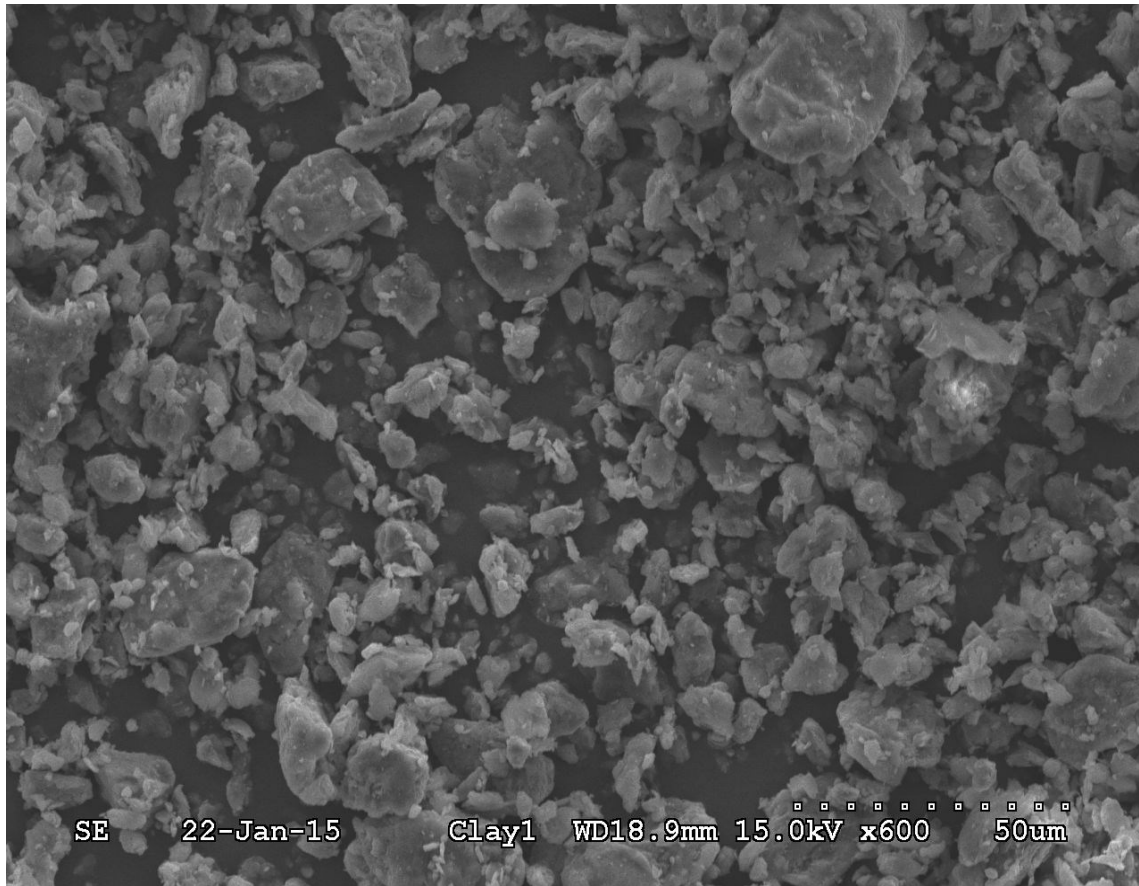


**Figure E.1 SEM Image of Original Sepiolite**



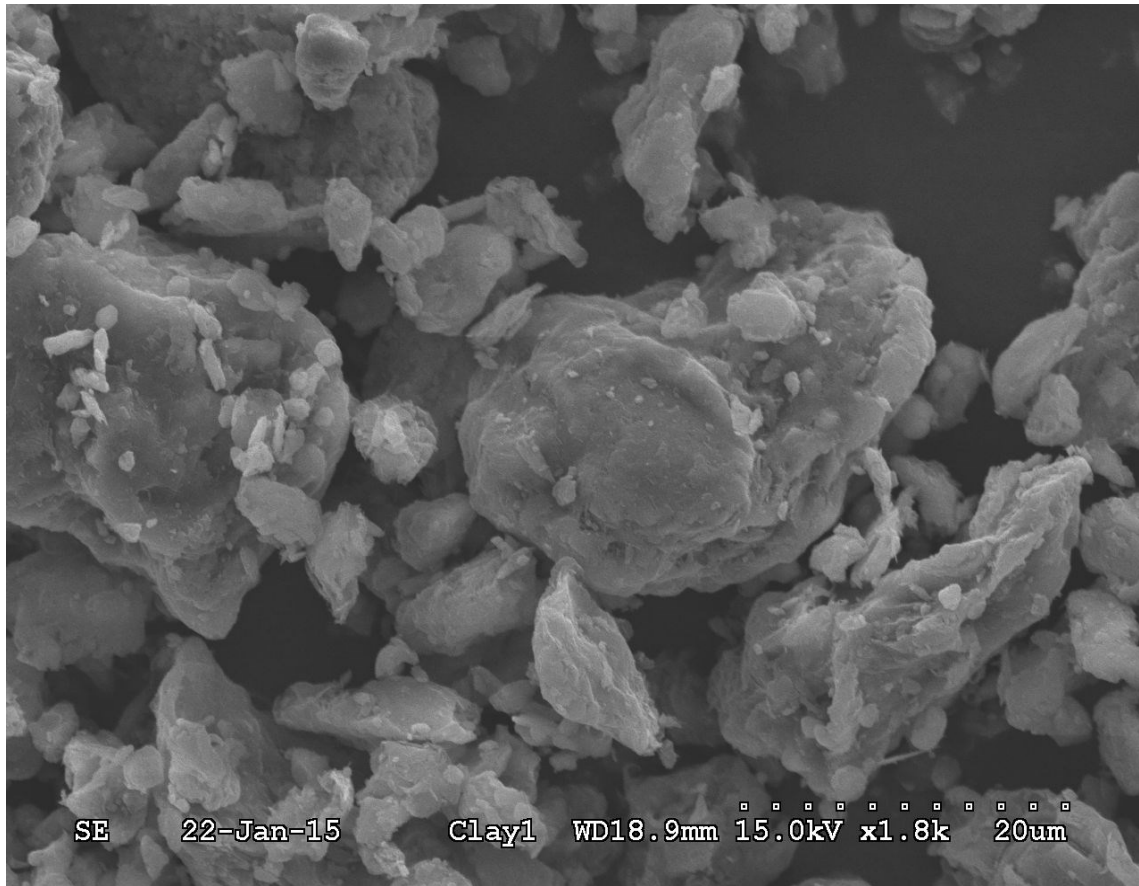


**Figure E.2 SEM Image of Original Sepiolite**

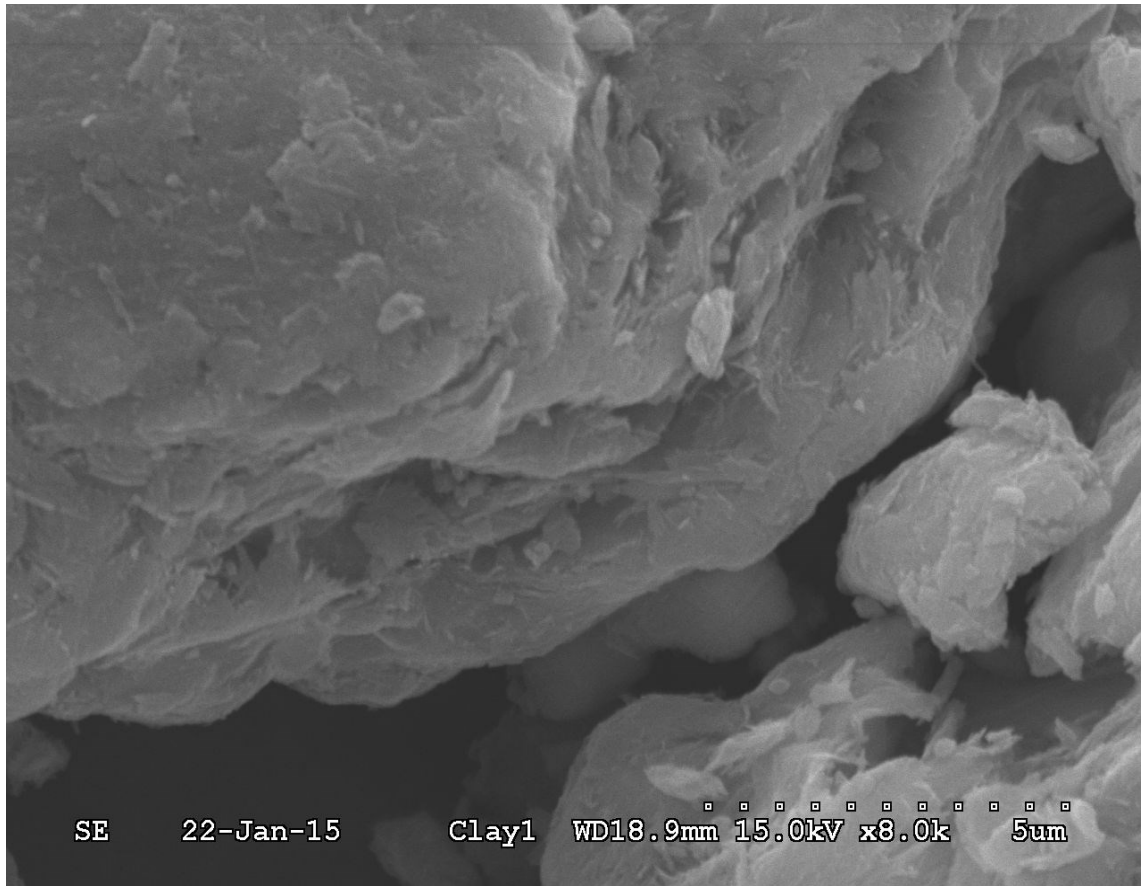


**Figure E.3 SEM Image of Original Sepiolite**

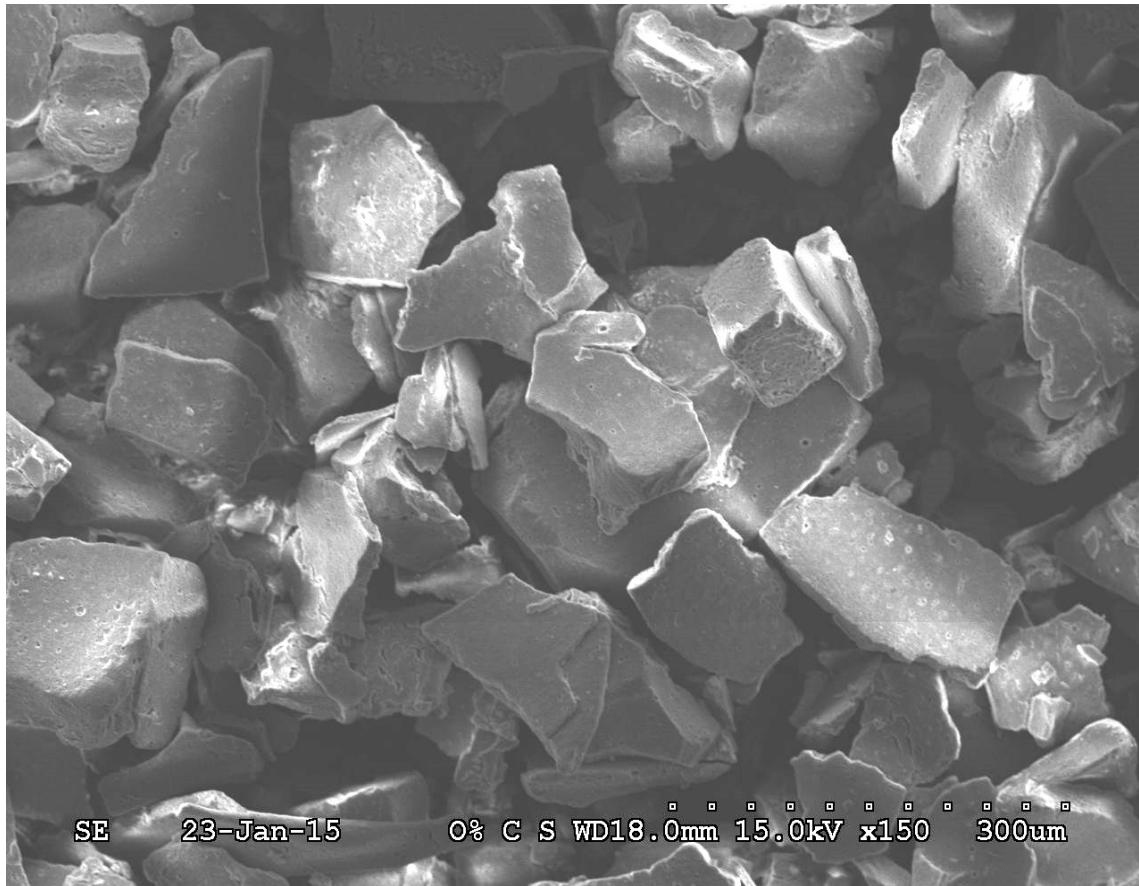


**Figure E.4 SEM Image of Greek Yogurt Whey Bottom Sediment Layer without Sepiolite**

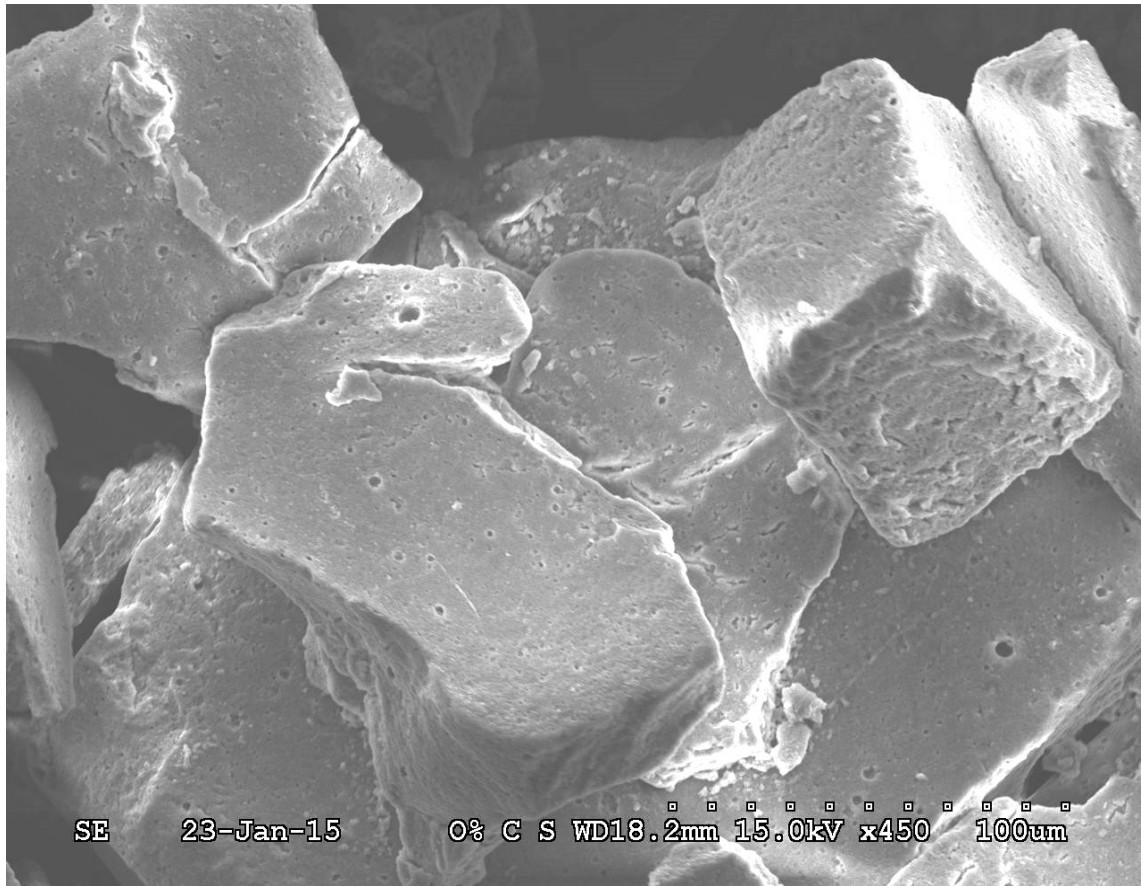


**Figure E.5 SEM Image of Greek Yogurt Whey Bottom Sediment Layer without Sepiolite**

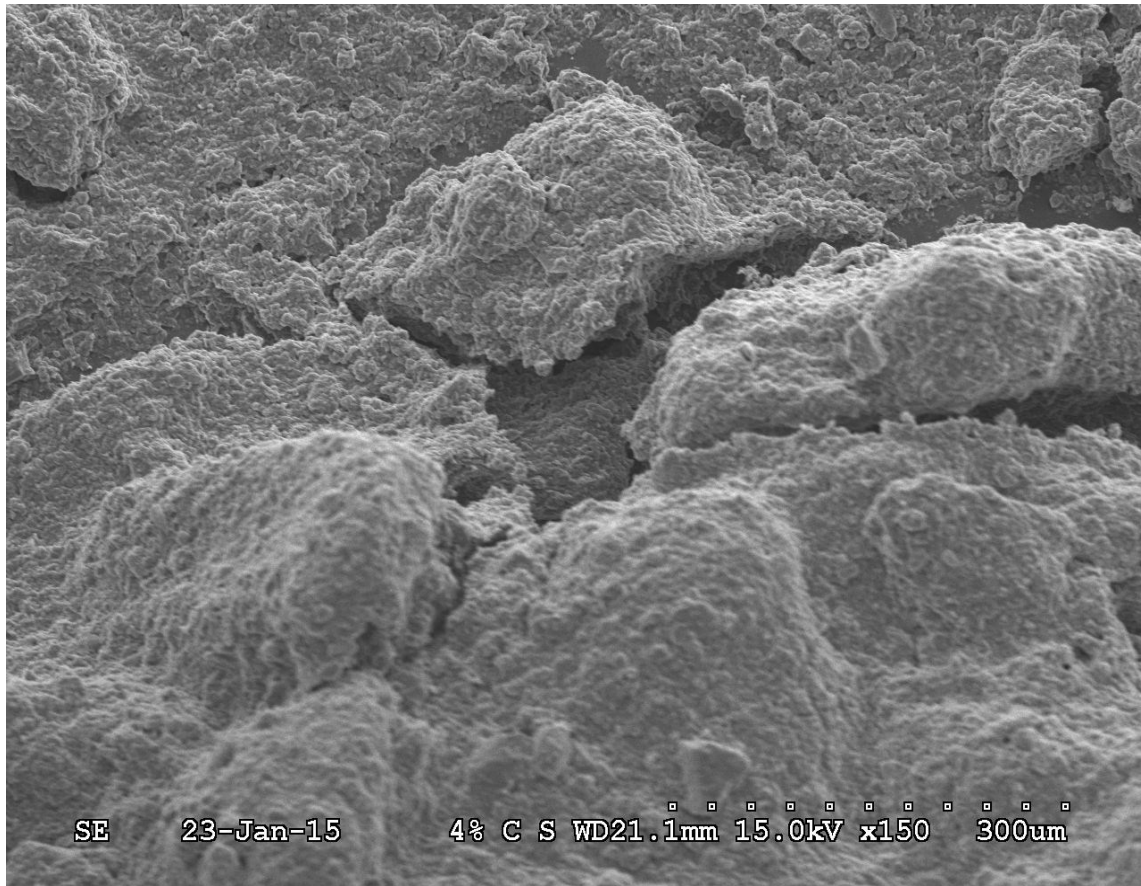


**Figure E.6 SEM Image of Sepiolite with Greek Yogurt Whey**

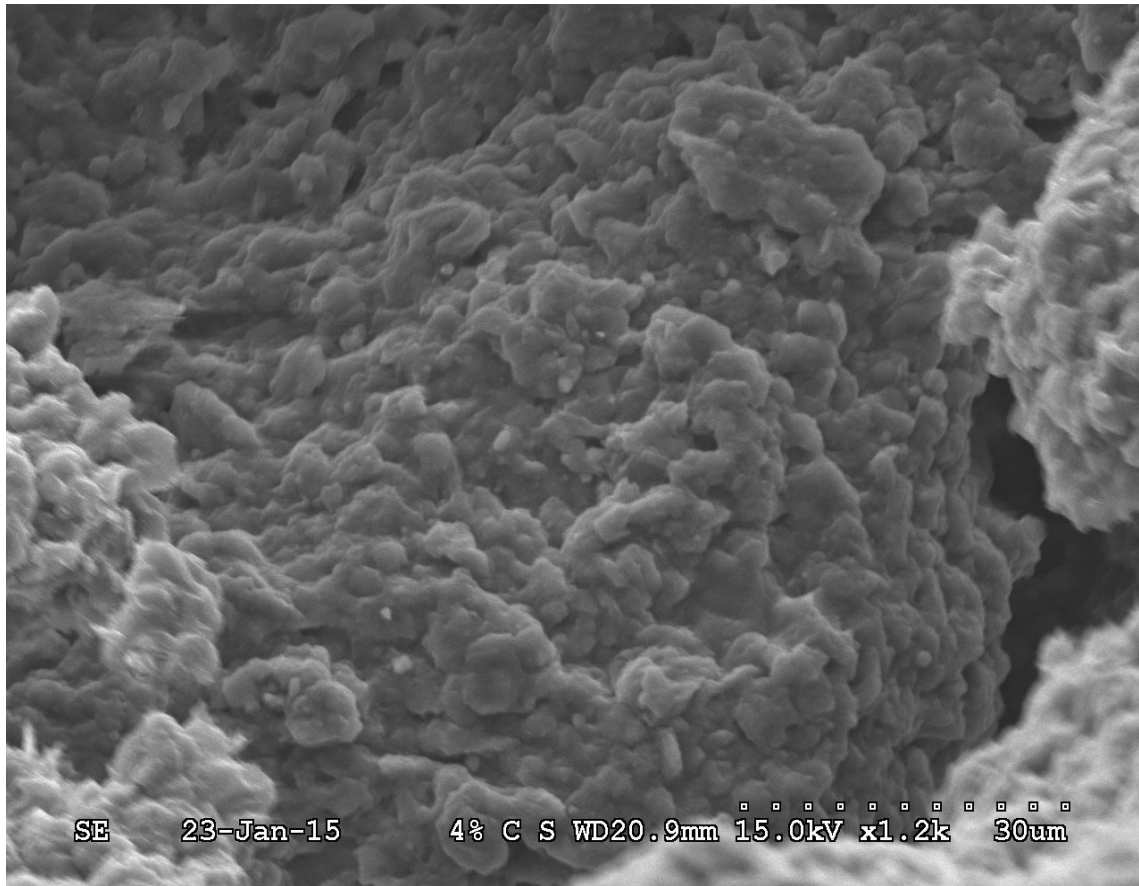


**Figure E.7 SEM Image of Sepiolite with Greek Yogurt Whey**

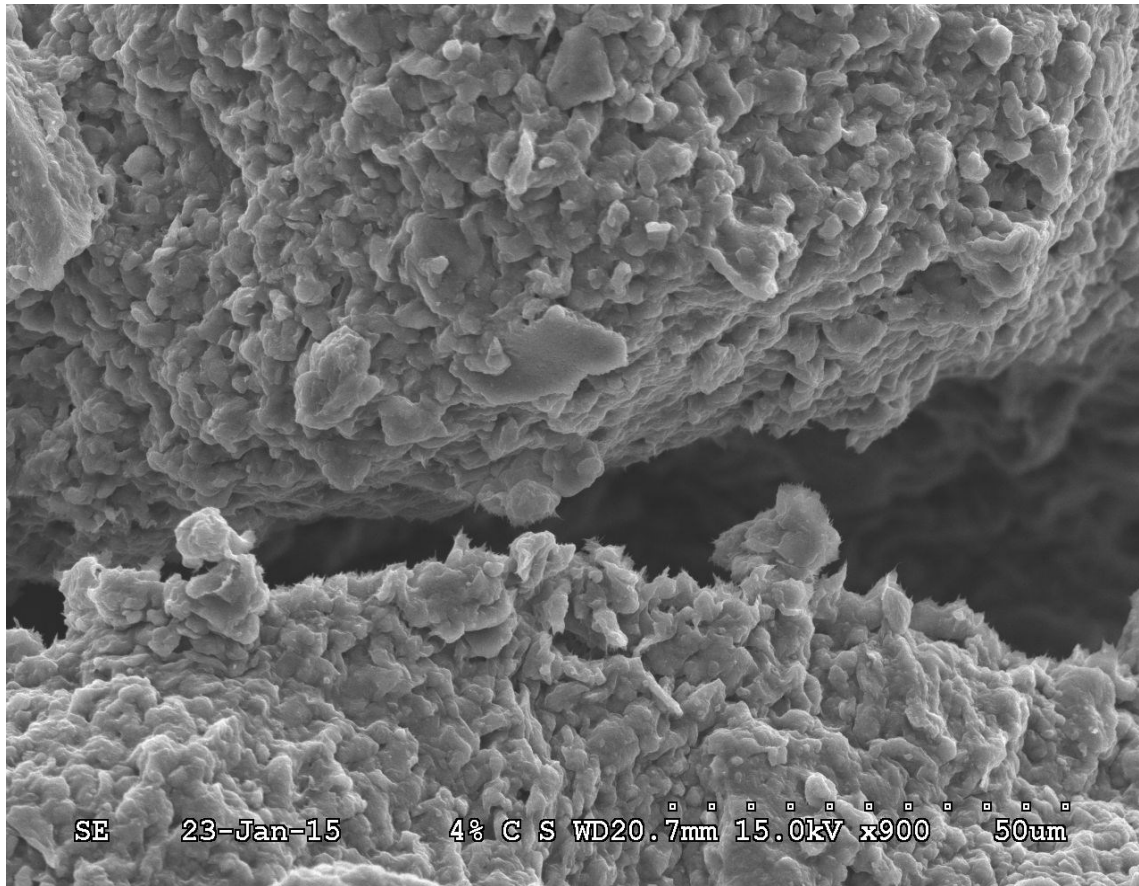


**Figure E.8 SEM Image of Sepiolite with Greek Yogurt Whey**

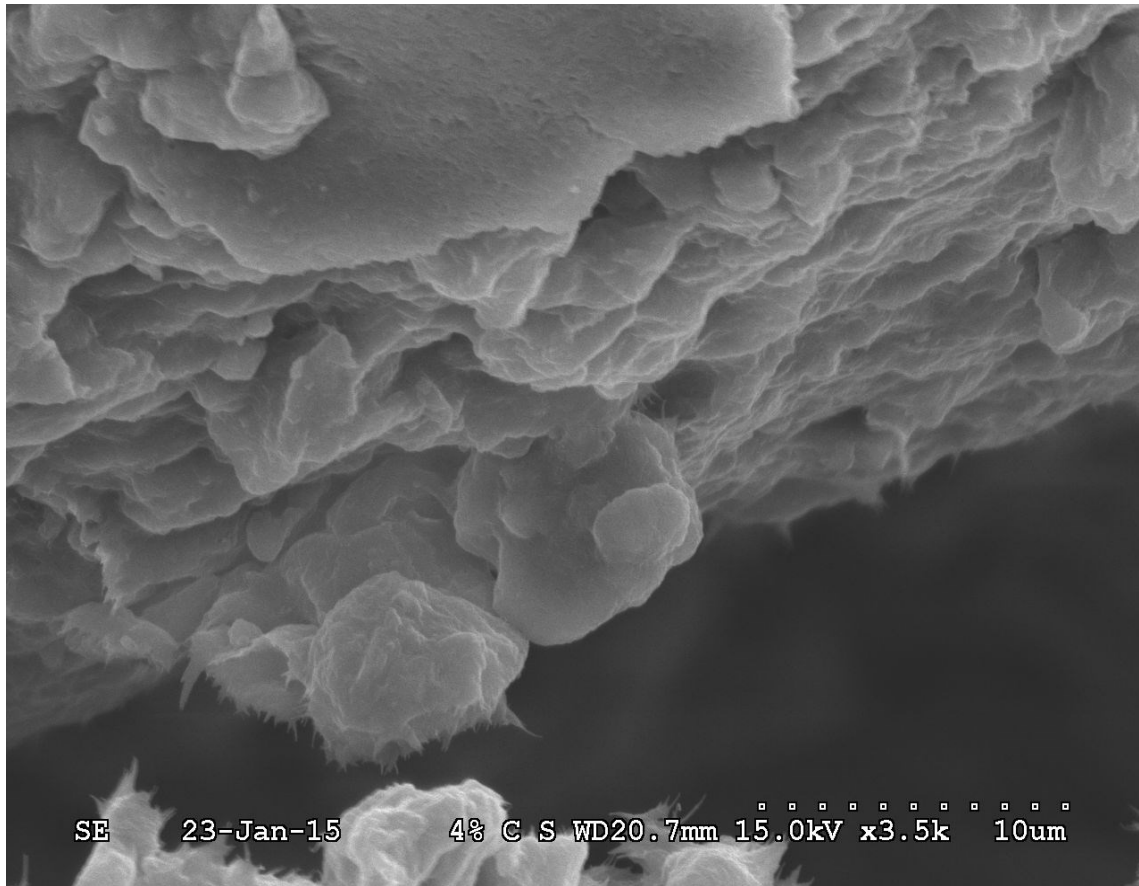


**Figure E.9 SEM Image of Sepiolite with Greek Yogurt Whey**



## **Appendix F - Images of Color Change in Greek Yogurt Whey Top Aqueous Layers from Sepiolite Addition for Chapter 3**

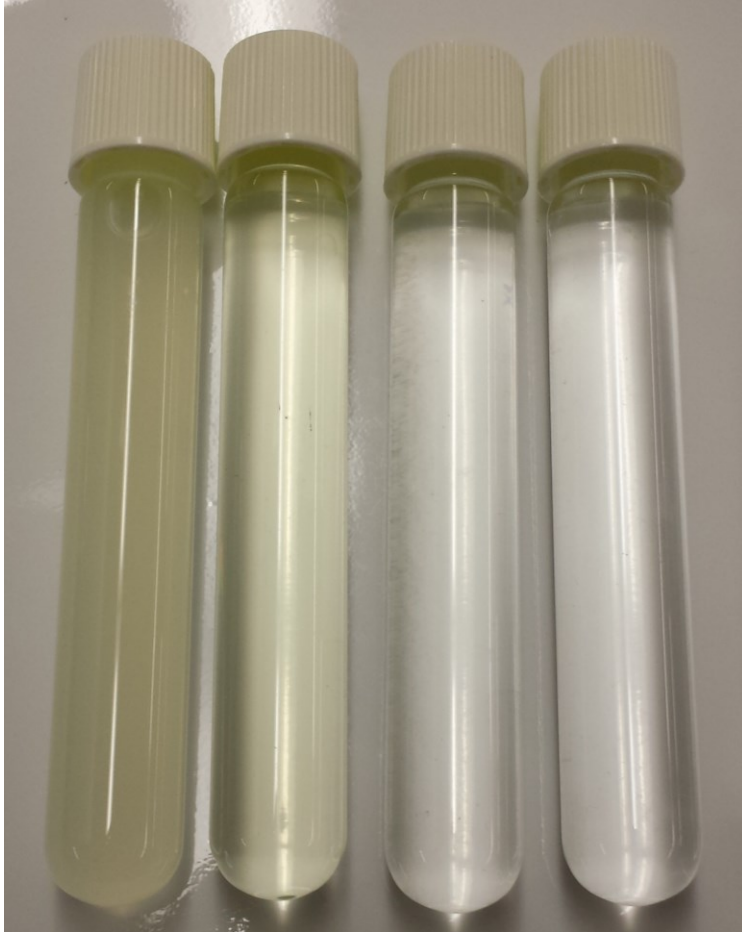


**Figure F.1 Image of Color Change in Greek Yogurt Whey Top Aqueous Layers from Sepiolite Addition for Chapter 3; from left to right: original Greek yogurt whey (GYW), 0g sepiolite per 100g GYW, 2g sepiolite per 100g GYW, and 4g sepiolite per 100g GYW**



**Figure F.2 Image of Color Change in Greek Yogurt Whey Top Aqueous Layers from Sepiolite Addition for Chapter 3; from left to right: centrifuged samples of 4g sepiolite per 100g Greek yogurt whey (GYW), 2g sepiolite per 100g GYW, and 0g sepiolite per 100g GYW**